

Julia Obmann, BSc

# **Disjoint Compatibility of Plane Perfect Matchings via other Graph Classes**

## **MASTER'S THESIS**

to achieve the university degree of  
Diplom-Ingenieurin  
Master's degree programme: Mathematics

submitted to

**Graz University of Technology**

### **Supervisor**

Assoc.Prof. Dipl.-Ing. Dr.techn. Oswin Aichholzer  
Institute for Softwaretechnology

Graz, September 2020

## **AFFIDAVIT**

I declare that I have authored this thesis independently, that I have not used other than the declared sources/resources, and that I have explicitly indicated all material which has been quoted either literally or by content from the sources used. The text document uploaded to TUGRAZonline is identical to the present master's thesis.

---

Date, Signature

# Acknowledgements

First of all I want to express my deepest gratitude to my parents. They did not only support me during my whole study and during the development of this thesis, but they always stand by my side in every sense as one of the most important people in my life. Very dear thanks to my little sister Nina who is always there for me if I need her, no matter what. Thanks as well to all other family members who always supported me on my way.

A big thanks to Alexandra Weinberger for the great and precise proof-reading of this thesis.

Thank you to my study colleagues with whom I spent many hours in the last years and among whom I found true friends.

Many thanks to all colleagues I got to know during the development of this thesis and with whom I already did research. I especially want to thank Birgit Vogtenhuber for the interesting conversations of scientific and non-scientific nature and my other co-authors Daniel Perz, Josef Tkadlec, Pavel Paták and Ruy Fabila-Monroy for the great collaboration.

Last but not least I want to express my infinite gratitude to my supervisor Oswin Aichholzer. He opened the world of discrete and computational geometry for me and through him I already got so many chances to do research in this area and get to know the work on this topics. Thank you a lot for this possibility and the many great conversations and experiences.

# Danksagung

Zuallererst will ich meinen Eltern meine tiefste Dankbarkeit aussprechen. Sie haben mich nicht nur während meines gesamten Studiums und während der Erstellung dieser Masterarbeit unterstützt, sondern stehen als eine der wichtigsten Personen in meinem Leben immer und in jeder Hinsicht an meiner Seite. Ganz lieben Dank an meine kleine Schwester Nina, die immer für mich da ist und ein offenes Ohr für mich hat, ganz egal worum es geht. Danke auch an alle anderen Familienmitglieder, die mich immer auf meinem Weg unterstützt haben.

Ein großes Danke an Alexandra Weinberger für das so tolle und genaue Korrekturlesen dieser Arbeit.

Danke an meine Studienkollegen, mit denen ich in den letzten Jahren so viele Stunden verbracht haben und unter denen ich wahre Freunde gefunden habe.

Vielen Dank an alle Kollegen, die ich während der Entstehung dieser Arbeit kennengelernt habe und mit denen ich schon gemeinsam geforscht habe. Besonders bedanken möchte ich mich bei Birgit Vogtenhuber für die interessanten Gespräche sowohl wissenschaftlicher als auch nichtwissenschaftlicher Natur und bei meinen anderen Koautoren Daniel Perz, Josef Tkadlec, Pavel Paták und Ruy Fabila-Monroy für die großartige Zusammenarbeit.

Zu guter Letzt will ich meinen unendlich großen Dank an meinen Betreuer Oswin Aichholzer ausdrücken. Durch ihn habe ich das Gebiet der algorithmischen Geometrie erst kennengelernt und bereits so viele Gelegenheiten bekommen, in diesem Bereich zu forschen und die Arbeit an diesen Themen kennenzulernen. Vielen Dank für diese Möglichkeit und für die vielen damit verbundenen Gespräche und Erlebnisse.

# Abstract

In this thesis we consider the set of all plane perfect matchings on  $2n$  points in convex position. We define several disjoint compatibility graphs such that each matching is a vertex in these graphs. Two such vertices are connected, if their matchings are both disjoint compatible to the same graph  $G$  of a given class, that is, the union of the matching and  $G$  is plane and edge-disjoint.

For the class of all plane spanning trees, we show that the disjoint compatibility graph of all matchings on a set of at least ten points is connected with constant diameter. The second approach is to define disjoint compatibility via plane Hamiltonian paths. In that case, the graph is not even connected when restricting to matchings with at least one disjoint compatible Hamiltonian path. Finally, we prove that all plane perfect matchings on at least ten points in convex position are connected via disjoint compatible caterpillar trees with maximum degree 3. The diameter for this compatibility graph is of size  $O(n)$ .

# Kurzfassung

In dieser Arbeit betrachten wir die Menge aller planen perfekten Matchings auf  $2n$  Punkten in konvexer Lage. Wir definieren verschiedene disjunkte Kompatibilitätsgraphen, wobei jedes Matching einen Knoten bildet. Zwei Knoten sind dabei verbunden, wenn die entsprechenden Matchings disjunkt kompatibel zum selben Graphen  $G$  einer gegebenen Klasse sind, das heißt, die Vereinigung eines Matchings mit  $G$  ist plan und kantendisjunkt.

Für die Klasse aller planen Spannbäume zeigen wir, dass der disjunkte Kompatibilitätsgraph aller Matchings auf einer Menge von mindestens zehn Punkten zusammenhängend mit konstantem Durchmesser ist. Als zweiten Ansatz definieren wir disjunkte Kompatibilität über plane Hamiltonpfade. In diesem Fall ist der Graph auch dann nicht zusammenhängend, wenn wir uns auf Matchings mit zumindest einem disjunkt kompatiblen Hamiltonpfad beschränken. Schließlich beweisen wir, dass alle planen perfekten Matchings auf zumindest zehn Punkten in konvexer Lage über disjunkt kompatible Raupenbäume mit Maximalgrad 3 zusammenhängend sind. Der Durchmesser für diesen Kompatibilitätsgraphen ist  $O(n)$ .

# Contents

<b>1</b>	<b>Introduction</b>	<b>8</b>
1.1	Compatibility . . . . .	8
1.2	Disjoint compatibility . . . . .	9
1.3	Compatibility via other graph classes . . . . .	10
<b>2</b>	<b>Disjoint tree-compatible matchings</b>	<b>11</b>
2.1	Basic definitions . . . . .	11
2.2	Upper bound for the diameter of the disjoint tree-compatibility graph . . . . .	12
2.3	Lower bound for the diameter of the disjoint tree-compatibility graph . . . . .	21
<b>3</b>	<b>Disjoint path-compatible matchings</b>	<b>32</b>
3.1	Basic definitions and special cases . . . . .	32
3.2	Plane perfect matchings with two semiears . . . . .	36
<b>4</b>	<b>Disjoint caterpillar-compatible matchings</b>	<b>54</b>
4.1	Basic definitions and general case . . . . .	54
4.2	Disjoint compatibility via one-legged caterpillars . . . . .	59
<b>5</b>	<b>Conclusion</b>	<b>62</b>
	<b>List of Figures</b>	<b>64</b>
	<b>List of Tables</b>	<b>69</b>
	<b>Bibliography</b>	<b>70</b>

# 1 Introduction

In this thesis we study different concepts of geometric compatibility between two plane perfect matchings, or to be more precise, compatibility between all plane perfect matchings on the same set  $S$  of points in the plane in general position. General position means that no three points are collinear. To begin with, we consider versions of compatibility, where the two matchings are directly compared with each other.

## 1.1 Compatibility

We only consider geometric graphs, that is, all edges are straight lines. We focus on matchings on our given point set  $S$ , more precisely, on (plane) perfect matchings.

**Definition 1.1.** A set of (plane) edges  $M$  on  $S$  is called *matching*, if every vertex in  $S$  is incident to at most one edge in  $M$ . If every vertex is incident to exactly one matching edge, then  $M$  is a *perfect matching*.

**Definition 1.2.** Two plane perfect matchings  $M$  and  $M'$  on  $S$  are called *compatible* if their union is also plane.

**Definition 1.3.** The *compatibility graph*  $\mathcal{M}(S)$  of a point set  $S$  is defined as follows:

- the set of vertices consists of all possible plane perfect matchings on  $S$



- two vertices are connected by an edge if and only if the respective matchings are compatible.

In [6], Hernando et al. consider a variation  $\mathcal{M}^*(S)$  of the compatibility graph  $\mathcal{M}(S)$ , where two vertices are adjacent if the symmetric difference of the respective matchings is a non-crossing cycle of length 4 in  $S$ . They prove that for a set  $S$  of  $2n$  points in convex position,  $\mathcal{M}^*(S)$  is connected with diameter  $n - 1$ . As a consequence, we can deduce that  $\mathcal{M}(S)$  is connected as well.

In 2005, Houle et al. extended the problem to point sets in general position and showed that  $\mathcal{M}^*(S)$  and therefore also  $\mathcal{M}(S)$  are connected for point sets in general position [7]. Furthermore, in [2] the diameter of  $\mathcal{M}(S)$  has been upper bounded by  $O(\log n)$ . A lower bound of  $\Omega(\log n / \log \log n)$  was obtained by Razen in [9].

## 1.2 Disjoint compatibility

**Definition 1.4.** Two plane perfect matchings  $M$  and  $M'$  on  $S$  which are compatible and in addition have no edge in common are called *disjoint compatible*.

The disjoint compatibility graph  $\mathcal{D}(S)$  can now be defined in the same way as the compatibility graph  $\mathcal{M}(S)$ .

**Definition 1.5.** The *disjoint compatibility graph*  $\mathcal{D}(S)$  of a point set  $S$  is defined as follows:

- the set of vertices is made up of all possible plane perfect matchings on  $S$
- two vertices are connected by an edge if and only if the respective matchings are disjoint compatible.

Aichholzer et al. give examples of isolated vertices in  $\mathcal{D}(S)$  for sets  $S$  of  $2n$  points where  $n$  is odd, namely those plane perfect matchings on convex point sets  $S$  consisting of only parallel matching edges as depicted in Figure 1.1 [2].

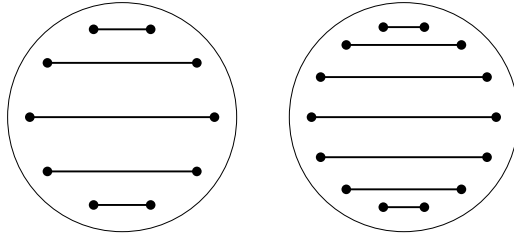


Figure 1.1: Plane perfect matchings on 10 and 14 points, respectively, with no disjoint compatible plane perfect matching.

For even  $n$ , the authors pose the conjecture that no such isolated vertices exist. Indeed, this was confirmed by Ishaque et al. in [8]. They show that every plane perfect matching on a set of  $2n$  points in general position obtains a disjoint compatible matching for all even  $n$ . However, in 2015 Aichholzer et al. could prove that for  $n \geq 3$ , the disjoint compatibility graph is always disconnected [1].

### 1.3 Compatibility via other graph classes

We next define alternative concepts of compatibility. The idea is to use a different graph class as an intermediate step in the following way: Two plane perfect matchings are considered compatible in that case if they are both disjoint compatible to the same graph of a fixed graph class. Note that they do not necessarily have to be disjoint compatible or even compatible to each other.

For the second graph class it makes sense to only consider classes of plane spanning graphs. Disjoint compatibility for two different graph classes is defined analogously to disjoint compatibility between two (plane perfect) matchings.

## 2 Disjoint tree-compatible matchings

This chapter is based on the paper 'Disjoint tree-compatible plane perfect matchings' presented at EuroCG 2020 [3].

### 2.1 Basic definitions

From now on let  $S$  be a set of  $2n$  points in the plane in convex position if not mentioned otherwise.

To begin with, we extend the definition of disjoint compatibility to arbitrary graphs.

**Definition 2.1.** Two plane graphs  $X$  and  $X'$  on  $S$  are called *disjoint compatible* if they have neither common nor crossing edges.

**Definition 2.2.** Let  $M, M'$  be two plane perfect matchings on  $S$ . If there exists a plane spanning tree  $T$  on  $S$  such that both  $M$  and  $M'$  are disjoint compatible to  $T$ , then  $M$  and  $M'$  are called *disjoint tree-compatible*.

**Definition 2.3.** The *disjoint tree-compatibility graph*  $G_{2n}$  is defined as follows:

- the set of vertices is made up of all possible plane perfect matchings on  $S$

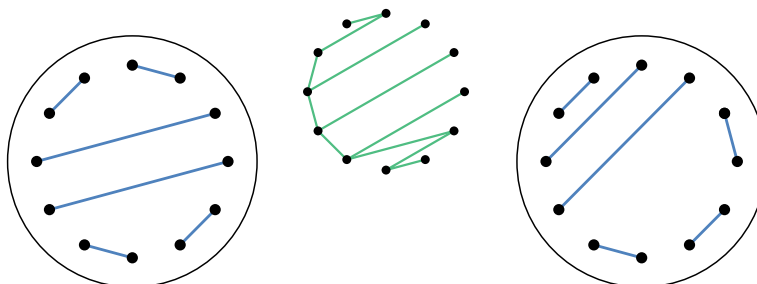


Figure 2.1: Two plane perfect matchings on the same set of twelve points in convex position (drawn in blue) which are disjoint tree-compatible. The complying disjoint compatible spanning tree is drawn in green.

- two vertices are connected by an edge if and only if the respective matchings are disjoint tree-compatible.

**Definition 2.4.** Edges spanned by two neighbouring points on the boundary of the convex hull of  $S$  are called *perimeter edges*; all other edges spanned by  $S$  are called *diagonals*.

**Definition 2.5.** A *perimeter matching* is a matching containing no diagonal. We label the sides of the convex hull of  $S$  alternately 'odd' and 'even'. Then the perimeter matching consisting of only odd perimeter edges is called *odd perimeter matching*, the one consisting of only even perimeter edges is likewise called *even perimeter matching*, see Figure 2.2.

## 2.2 Upper bound for the diameter of the disjoint tree-compatibility graph

In this chapter we show that for convex point sets  $S$  of at least ten points, the disjoint compatibility graph  $G_{2n}$  is connected and we further prove that the diameter is upper bounded by 5. The idea is that any matching on  $S$  has small

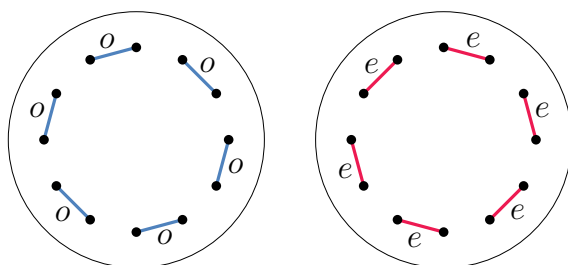


Figure 2.2: The two perimeter matchings on a set of twelve points. The odd perimeter matching is drawn in blue and the even perimeter matching is drawn in red.

distance to one of the two perimeter matchings and those themselves are close to each other in  $G_{2n}$ .

First we introduce key notions of a semicycle, a cycle of edges and a rotation.

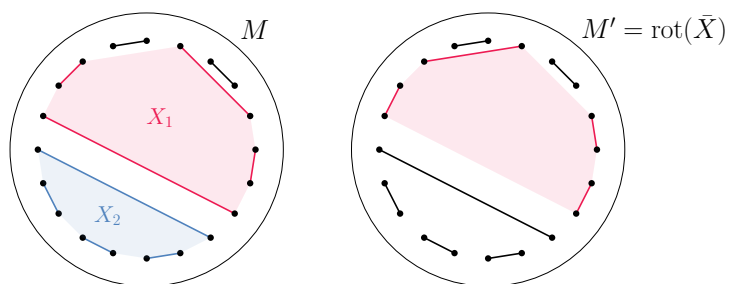


Figure 2.3: Left: A matching  $M$  with two semicycles  $X_1$  (red edges) and  $X_2$  (blue edges) and their convex hulls. The corresponding cycle  $\bar{X}_1$  is an inside 4-cycle, since the boundary of the red shaded area contains at least two (in fact three) diagonals. The cycle  $\bar{X}_2$  is a 4-ear. Right: The matching  $M'$  resulting from rotating the cycle  $\bar{X}_1$ .

**Definition 2.6.** Let  $M$  be a plane perfect matching on  $S$ .

- A set  $X$  of  $k \geq 2$  matching edges is called a  $k$ -semicycle if the interior of the convex hull of  $X$  does not intersect any edges of  $M$ .
- Given a  $k$ -semicycle  $X$ , the boundary of its convex hull (including the non-matching edges) is called its  $k$ -cycle and denoted by  $\bar{X}$ .

- A  $k$ -cycle  $\bar{X}$  is called an *inside  $k$ -cycle* (or just an *inside cycle*) if  $\bar{X}$  contains at least two diagonals, otherwise it is called a  *$k$ -ear* (or just an *ear*).
- Finally, given a semicycle  $X$  in a matching  $M$ , we can obtain a matching  $M' = \text{rot}(\bar{X})$  by *rotating* the cycle  $\bar{X}$ , that is, by removing from  $M$  the edges in  $X$  and adding the edges in  $\bar{X} \setminus X$ .

We will now show that arbitrary many inside cycles can be simultaneously rotated in one step.

**Lemma 2.7.** Let  $M$  and  $M'$  be two matchings whose symmetric difference is a union of disjoint inside cycles. Then  $M$  and  $M'$  are disjoint tree-compatible to each other.

*Proof.* Let  $M$  and  $M'$  be two matchings and first assume that their symmetric difference is a single inside cycle  $C$  (such that  $C_1$  is a semicycle of  $M$  and  $C_2 = C \setminus C_1$  is a semicycle of  $M'$ ; cf. Figure 2.4(a)). We need to show that there exists a tree disjoint from  $M \cup M'$  and compatible with both matchings.

By assumption,  $C$  has at least two diagonals (which do not necessarily lie in  $M$  or  $M'$ ). Pick two endpoints  $u, v$  on two different diagonals of  $C$  such that  $u$  and  $v$  are not adjacent vertices of  $C$ . Triangulate the inside of  $C$  such that  $u$  and  $v$  are the only ears of the triangulation (this is possible since  $C$  is convex and  $u, v$  are not consecutive). The set  $D$  of diagonals in this triangulation is a spanning tree of all the points of  $C$  except  $u$  and  $v$  (see Figure 2.4(b)).

Now, for each outside part  $P_i$  determined by  $C$  (containing the corresponding boundary diagonal of  $C$  as in Figure 2.4(c)), extend the set of edges in  $M_i := (M \cup C) \cap P_i$  to a triangulation, call it  $T_i$  (Figure 2.4(d)). We claim that the added edges  $A_i$  span the whole part  $P_i$ : Indeed, the whole  $T_i$  is connected and each edge  $e \in M_i$  is a side of a triangle whose other two edges were added (no two edges in  $M_i$  share an endpoint), hence removing  $e$  does not disconnect  $T_i$ . Moreover,  $D \cup A_i$  is connected, since  $A_i$  connects to both endpoints of the shared diagonal and  $D$  misses at most one of them. This is true for all outside parts  $P_i$ , hence  $D \cup \bigcup_i A_i$  is a planar spanning graph that is edge-disjoint from

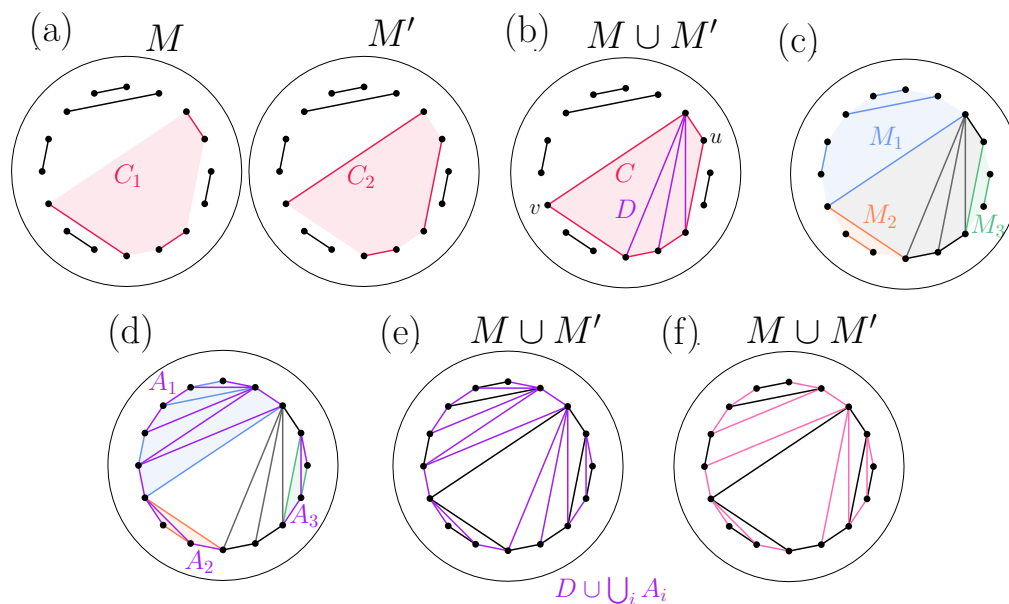


Figure 2.4: (a) Two plane perfect matchings on the same convex point set differing at a single inside cycle (shaded in red). (b) Triangulation of the cycle  $C$  such that  $u$  and  $v$  are the only two ears. The added diagonals  $D$  are drawn in purple. (c) Three outside parts  $P_1$ ,  $P_2$  and  $P_3$  (shaded) and the respective edge sets  $M_1$ ,  $M_2$  and  $M_3$  (coloured). (d) Triangulation  $T_i = M_i \cup A_i$  of the outside parts; the added edges  $A_i$  are drawn in purple. (e) The union of  $D$  and all  $A_i$  results in a planar spanning graph which contains a spanning tree (depicted in (f) in pink).

$M \cup C$  and compatible with it (Figure 2.4(e)). Breaking cycles one by one we eventually obtain a spanning tree (Figure 2.4(f)).

When the symmetric difference consists of multiple disjoint inside cycles, in the first step we triangulate each of them separately. The second step then works in the same way.  $\square$

As we covered all inside cycles, we now consider ears and show that sufficiently large ears can be rotated in at most three steps.

**Lemma 2.8.** Let  $M$  and  $M'$  be two matchings whose symmetric difference is a  $k$ -ear with  $k \geq 6$ . Then  $M$  and  $M'$  have distance at most 3 (in  $G_{2n}$ ).

*Proof.* The idea of the proof is to perform three rotations of inside cycles. We proceed as in Figure 2.5:

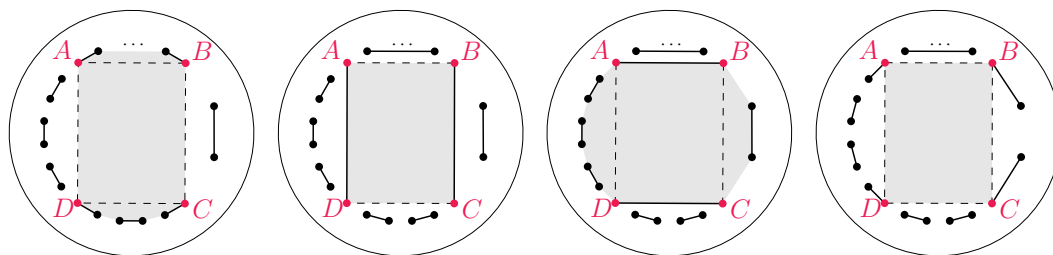


Figure 2.5: Intermediate steps for the rotation of a  $k$ -ear with  $k \geq 6$ .

First we find 4 points  $A, B, C, D$  on the ear such that each of the four arcs  $\widehat{AB}, \widehat{BC}, \widehat{CD}, \widehat{DA}$  of the ear contains a positive even number of points in its interior. W.l.o.g. the points  $A, B$  are matched inside  $\widehat{AB}$  and  $C, D$  are matched inside  $\widehat{CD}$ . We do the following three steps: Rotate  $\widehat{ABCD}$ , rotate a 2-cycle  $ABCD$ , rotate  $\widehat{BCDA}$ . Since each arc initially contained at least two points, each step rotates an inside cycle and it is easily checked that this transforms  $M$  into  $M'$ .  $\square$

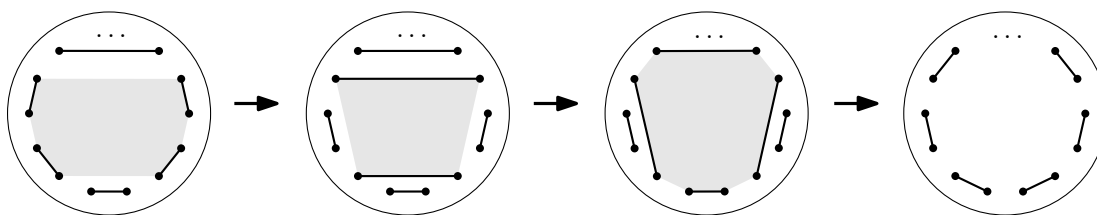


Figure 2.6: Rotation of a 6-ear in 3 steps (in each step we rotate the grey inside cycle).

**Theorem 2.9.** For  $2n \geq 10$ , the disjoint compatibility graph  $G_{2n}$  is connected and  $\text{diam}(G_{2n}) \leq 5$ .



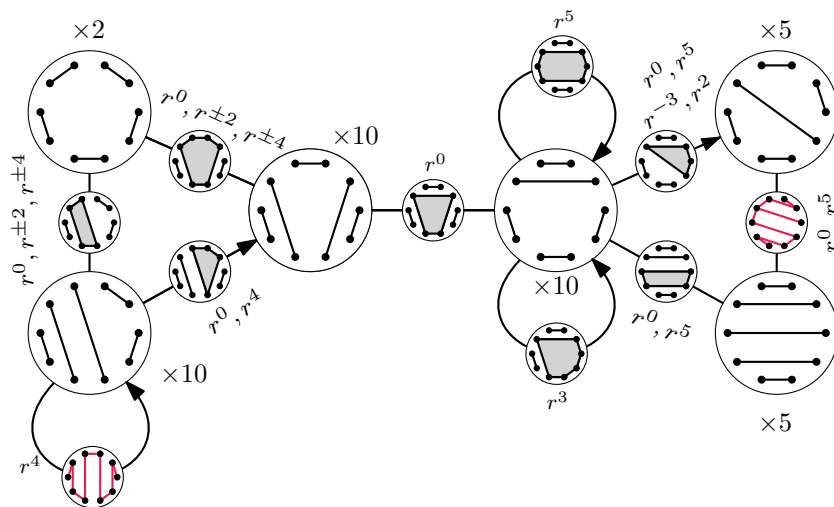


Figure 2.7: Schematic depiction of the whole graph  $G_{10}$ . The letter  $r$  stands for a possible rotation by  $2\pi/10$ . Going against the arrows rotates in opposite direction. Next to each vertex, the number of different matchings resulting from rotations is indicated. The edges indicate either the rotation of an inside cycle (in gray), or a compatible spanning tree (red).

*Proof.* For  $2n = 10$ , this is essentially depicted in Figure 2.7: If we want to find a path between rotated version of some nodes, we just need to find a walk in the picture along which the rotations compose to the desired value.

Now assume  $2n \geq 12$ . The idea is the following: between each matching and either one or both perimeter matchings as well as between the two perimeter matchings itself we find short sequences of disjoint tree-compatible matchings with a symmetric difference of only disjoint inside cycles.

We colour the perimeter alternately in blue and red and refer to the odd (resp. even) perimeter matching as the blue perimeter matching  $B$  (resp. red perimeter matching  $R$ ). Moreover, for a fixed matching  $M$ , let  $d_{\min}(M) = \min\{\text{dist}(M, B), \text{dist}(M, R)\}$  and  $d_{\max}(M) = \max\{\text{dist}(M, B), \text{dist}(M, R)\}$  be the distance from  $M$  to the closer and the further perimeter matching, respectively. Since by Lemma 2.8 we have  $\text{dist}(B, R) \leq 3$ , it suffices to show that the non-perimeter matchings can be split into three classes  $S_1, S_2, S_3$  with the

following properties (see Figure 2.8):

1.  $\forall M \in S_1$  we have  $d_{\min}(M) \leq 1$  (and hence  $d_{\max}(M) \leq 1 + 3 = 4$ );
2.  $\forall M \in S_2$  we have  $d_{\min}(M) \leq 2$  and  $d_{\max}(M) \leq 3$ ;
3.  $\forall M \in S_3$  we have  $d_{\max}(M) \leq 3$  and  $\forall M, M' \in S_3$  we have  $\text{dist}(M, M') \leq 4$ .

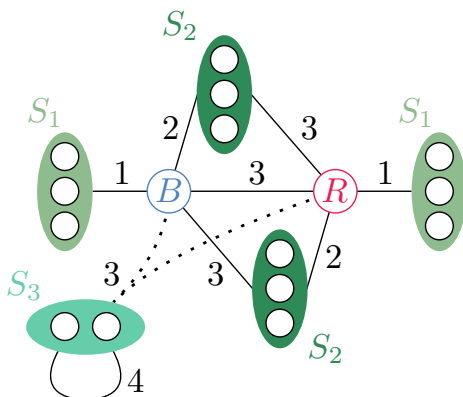


Figure 2.8: All matchings are sufficiently close to the blue (odd) perimeter matching  $B$  and/or to the red (even) perimeter matching  $R$ .

Fix a matching  $M$ . It consists of a number (possibly zero) of diagonals, odd perimeter edges (shown in blue), and even perimeter edges (shown in red). The convex hull of  $S$  is split by the diagonals into several polygons, each of them corresponding to a cycle. The dual graph  $D(M)$  of these polygons is a tree. Its leaves correspond to ears and the interior nodes correspond to inside cycles. Since the diagonals of  $M$  split the perimeter into (possibly empty) arcs that alternately consist of only red and only blue sides, the nodes of the tree can be properly two-coloured in blue and red by the colour of the perimeter edges of the corresponding polygons (see Figure 2.9).

Now we distinguish four cases based on what the dual tree  $D(M)$  looks like. Let  $b$  and  $r$  be the number of leaves in  $D(M)$  coloured blue and red, respectively. Wlog assume  $b \geq r$ .

- $b \geq 1, r = 0$ : If  $b = 1$  then  $M = B$ . Otherwise, we simultaneously rotate all red inside cycles. This removes all diagonals, we reach  $B$  in 1 step and we put  $M$  into  $S_1$ .

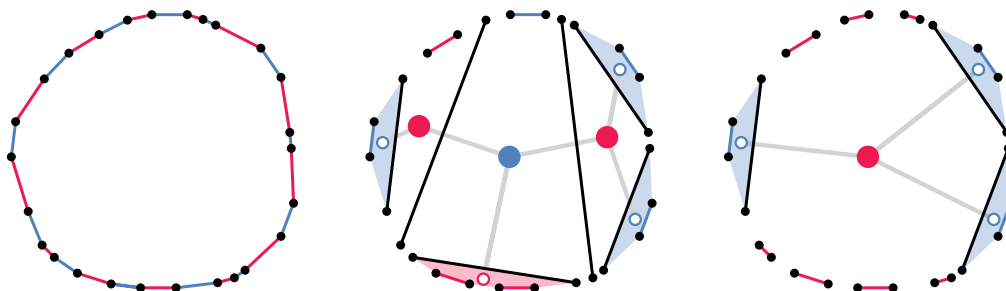


Figure 2.9: For a fixed matching  $M$ , we colour the perimeter edges alternately in blue (odd edges) and red (even edges). The colouring extends to a proper colouring of a tree  $D(M)$  that is dual to  $M$ . In the shown example, rotating the inside cycle corresponding to the blue interior node of  $D(M)$  creates a tree which leaves all have the same colour.

- $b \geq 2, r \geq 2$ : We can get to  $B$  in 2 steps: First, simultaneously rotate all blue inside cycles (this removes all diagonals except the ones separating blue leaves of  $D(M)$ ). Then rotate the (only, red) inside cycle. Similarly, we can reach  $R$  in 2 steps, hence  $M$  can go to  $S_2$ . (This case can only occur when  $2n \geq 16$ .)
- $b \geq 2, r = 1$ : See Figure 2.10. In the first step, rotate all blue inside cycles to get  $b \geq 2$  blue leaves and one (red) inside cycle. To get to  $B$ , rotate the inside cycle ( $\leq 2$  steps total). To get to  $R$ , note that the original diagonal that cut off the red leaf disappeared in the first step. Thus it was rotated out and we must now have at least  $1 + 1 + 1 \geq 3$  consecutive red sides, say  $e, f, g$ . Rotate the inside without  $e$  and  $g$  and then rotate

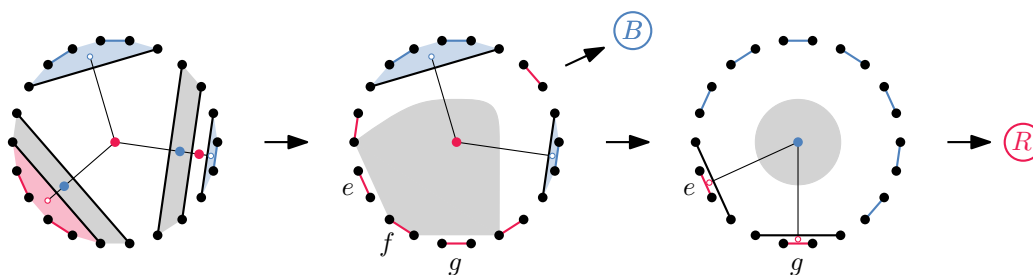


Figure 2.10: When  $b \geq 2$  and  $r = 1$  we can get to  $B$  in 2 steps and to  $R$  in 3 steps.

the inside. This gets to  $R$  in 3 steps, hence  $M$  can go to  $S_2$ . (This case can only occur when  $2n \geq 14$ .)

- $\underline{b = 1, r = 1}$ : In the first step, rotate all blue inside cycles. If the diagonal that cuts off the blue leaf is not there yet, push it to a side by rotating the whole blue ear without one blue perimeter edge (see Figure 2.11(a)). Note that this is simply a rotation of an inside cycle. Since  $2n \geq 10$ , we have at least 3 consecutive red edges and, as in the previous case, we can thus reach  $R$  in two more steps (for a total of 3 steps). For  $B$ , we can proceed in the same way, therefore we aim to put  $M$  into  $S_3$ .

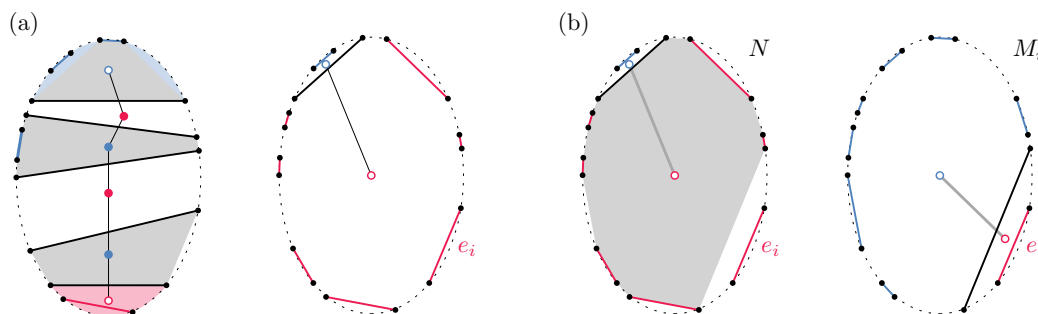


Figure 2.11: Intermediate steps for the case  $b = 1$  and  $r = 1$ .

For that, we need to check that any two such matchings are in distance at most 4 apart. To that end, it suffices to check that any two matchings  $N, N'$  with one diagonal that cuts off a single blue perimeter edge are in distance at most  $4 - 1 - 1 = 2$  apart. This is easy (see Figure 2.11(b)): Label the  $n$  red perimeter edges by  $e_1, \dots, e_n$  and for each  $i = 1, \dots, n$ , denote by  $M_i$  the matching with one diagonal that cuts off the perimeter edge  $e_i$ . We claim that some  $M_i$  is adjacent to both  $N$  and  $N'$ . In fact, we claim that  $N$  is adjacent to at least  $n - 2$  of the  $n$  matchings  $M_i$ . Indeed, for any of the  $n - 2$  red sides  $e_i$  present in  $N$ , we can rotate the (inside) cycle consisting of the red leaf of  $D(N)$  without  $e_i$ . The same holds for  $N'$ . Since for  $2n \geq 10$ , we have  $(n - 2) + (n - 2) > n$ , there is a matching  $M_i$  adjacent to both  $N$  and  $N'$ .

□

## 2.3 Lower bound for the diameter of the disjoint tree-compatibility graph

Since the diameter of  $G_{2n}$  has a constant upper bound, it seems reasonable to also ask for a best possible lower bound.

As for the upper bound, we start with some definitions as we introduce notions of *inside semicycles* and *semiears* for semicycles in the same way as we defined *inside cycles* and *ears* for cycles in 2.6:

**Definition 2.6.** Let  $M$  be a plane perfect matching on  $S$ .

- A set  $X$  of  $k \geq 2$  matching edges is called a *k-semicycle* if the interior of the convex hull of  $X$  does not intersect any edges of  $M$ .
- Given a  $k$ -semicycle  $X$ , the boundary of its convex hull (including the non-matching edges) is called its *k-cycle* and denoted by  $\bar{X}$ .
- A  $k$ -cycle  $\bar{X}$  is called an *inside k-cycle* (or just an *inside cycle*) if  $\bar{X}$  contains at least two diagonals, otherwise it is called a *k-ear* (or just an *ear*).
- Finally, given a semicycle  $X$  in a matching  $M$ , we can obtain a matching  $M' = \text{rot}(\bar{X})$  by *rotating* the cycle  $\bar{X}$ , that is, by removing from  $M$  the edges in  $X$  and adding the edges in  $\bar{X} \setminus X$ .

**Definition 2.10.** Let  $M$  be a matching on  $S$ . A  $k$ -semicycle  $X$  is called an *inside k-semicycle* (or just an *inside semicycle*) if  $\bar{X}$  contains at least two diagonals, otherwise it is called a *k-semiear* (or just a *semiear*).

**Definition 2.11.** Let  $M$  and  $M'$  be two matchings in  $S$ . A *boundary area with  $k$  points* is an area within the convex hull of  $S$  restricted by edges in  $M$  and  $M'$  such that the matching edges intersect at least once and the points on the boundary of the area are adjacent on the boundary of the convex hull of  $S$ ; see Figure 2.12.

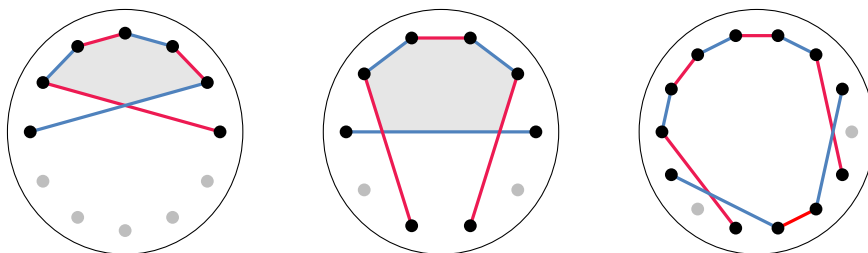


Figure 2.12: Boundary areas with five points (left) and four points (middle). The drawing on the right does not show a boundary area; not all points are neighbouring on the convex hull of  $S$ .

**Definition 2.12.** A matching  $M$  on a set of  $4k$  points is called a *2-semiear matching* if it consists of exactly  $k$  2-semiears and an inside  $k$ -semicycle. A matching  $M$  on a set of  $4k + 2$  points is called a *near-2-semiear matching* if it consists of exactly  $k$  2-semiears and an inside  $(k + 1)$ -semicycle.

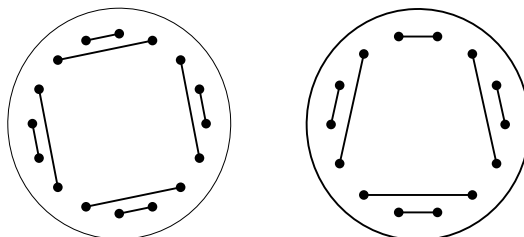


Figure 2.13: Left: A 2-semiear matching. Right: A near-2-semiear matching.

**Remark 2.13.** Analogous to perimeter matchings we can distinguish between odd and even 2-semiear matchings, according to the values taken by the respective perimeter edges.

**Lemma 2.14.** Let  $M, M'$  be two matchings whose symmetric difference is an ear or a boundary area with at least three points. Then  $M$  and  $M'$  are not disjoint tree-compatible to each other.

*Proof.* We consider two matchings  $M$  and  $M'$  creating a  $k$ -ear and we call the respective polygon  $P$  (cf. Figure 2.14). The proof for a boundary area with at least three points works in a similar way.

If the two matchings are disjoint tree-compatible, we can draw an edge-disjoint tree in  $S$ . Let  $p_1$  and  $p_2$  be the two endpoints of the diagonal in the ear. Any other point in  $P$  cannot be directly connected to a point outside  $P$  via a tree edge, therefore at least  $k - 2$  tree edges need to lie within  $P$  (if  $p_1$  and  $p_2$  are connected to each other outside  $P$ ; otherwise even  $k - 1$  tree edges are needed). However, by planarity there can be at most  $k - 3$  edges in a polygon spanned by  $k$  points, which leads to a contradiction.  $\square$

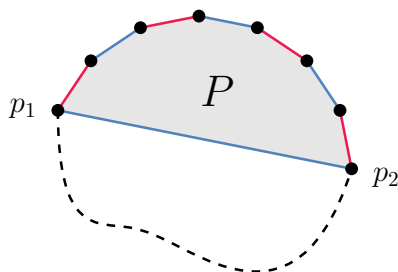


Figure 2.14: Two matchings  $M$  and  $M'$  (depicted in red and blue) creating an ear. The points  $p_1$  and  $p_2$  might be connected by a spanning tree outside the ear.

**Lemma 2.15.** Let  $M$  be a matching disjoint tree-compatible to an even 2-semi-ear-matching. Then  $M$  contains no odd perimeter edge.

*Proof.* We prove the statement by contradiction and assume that there exists a disjoint tree-compatible matching  $M$  which contains at least one odd perimeter edge. This matching edge connects one endpoint of a perimeter edge with its neighbouring vertex (matched by a diagonal in the 2-semi-ear matching), see Figure 2.15. We distinguish between the cases where the other endpoint of the perimeter edge is matched to (in  $M$ ). If it is matched with the same diagonal of the 2-semi-ear, the two matchings create an ear, a contradiction to Lemma 2.14 (cf. Figure 2.15 on the left). Otherwise, this matching edge intersects with the

diagonal of the 2-semiar matching. Therefore it creates a boundary area with three points, which is a contradiction to Lemma 2.14 (cf. Figure 2.15 on the right).  $\square$

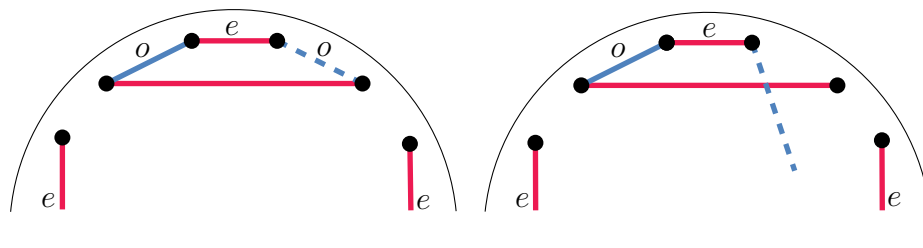


Figure 2.15: An (even) 2-semiar matching drawn in red and a blue matching with at least one odd perimeter edge; on the left the blue matching creates a cycle with the red matching, on the right a boundary area with three points occurs.

**Lemma 2.16.** Let  $M$  be a matching disjoint tree-compatible to a near-2-semiar-matching  $M'$  consisting of  $k$  even and one odd perimeter edge. Then  $M$  contains at most one odd perimeter edge (the one in  $M'$ ).

*Proof.* Let  $M'$  be a matching disjoint tree-compatible to a near-2-semiar matching  $M$  as defined in the statement. All but one of the odd perimeter edges would connect an even perimeter edge with its diagonal in a 2-semiar, therefore they cannot be contained in  $M'$  as shown in the proof of Lemma 2.15. Consequently, there is at most one odd perimeter edge in  $M'$  (which is exactly the odd perimeter edge in  $M$ ).  $\square$

**Lemma 2.17.** Let  $M$  and  $M'$  be two disjoint tree-compatible matchings. Then  $M$  and  $M'$  have at least two perimeter edges in common.

*Proof.* Let  $M'$  be a matching disjoint tree-compatible to  $M$ . First of all, we consider the case that  $M$  is a perimeter matching, w.l.o.g.  $M$  is the even perimeter matching. Our claim is that  $M'$  has no odd perimeter edge. This is



easy to see since any number of odd perimeter edges in  $M'$  creates an ear with  $M$ . Thus the two matchings cannot be disjoint tree-compatible to each other, which is a contradiction to the assumption. Therefore we can conclude that our statement holds for perimeter matchings since every matching contains at least two perimeter edges. (Consider the dual graph where the areas defined by matching edges correspond to points and two points are connected if and only if the two areas are separated by a matching edge. This graph forms a tree where semiears in the matching correspond to leaves in the tree.)

All other matchings have at least two semiears and we distinguish different cases.

Case 1: There exist two semiears of size  $\geq 3$  in  $M$

Our claim is that at least one of the perimeter edges of each semiear lies in  $M'$ . We consider one semiear and assume to the contrary that none of the perimeter edges of this semiear lies in  $M'$ .

W.l.o.g. we assume that the semiear is even. Thus by assumption, every vertex of this semiear is either matched by an odd perimeter edge or by a diagonal in  $M'$ . If all points in the semiear are matched by odd perimeter edges in  $M'$ , we get an ear contradicting Lemma 2.14 (cf. Figure 2.16 (a)).

If two points in the semiear are matched with each other by a diagonal (in  $M'$ ), the other points (in the semiear) are separated into two sets. Those on the side with just perimeter edges have to be matched with each other in  $M'$ , otherwise  $M'$  would intersect itself. We can iteratively shrink this side, until the remaining points are all matched by odd perimeter edges. This again creates an ear (cf. Figure 2.16 (b)).

Otherwise, at least one diagonal in  $M'$  intersects the diagonal (in  $M$ ) of the semiear, starting at an endpoint of an even perimeter edge. If the other endpoint of this edge is matched by an odd perimeter edge in  $M'$ , we get a boundary area with at least four points. Therefore, no spanning tree can be drawn and the matchings are not disjoint tree-compatible (cf. Figure 2.16 (c)).

If the other endpoint of the even perimeter edge is also matched by a diagonal in  $M'$ , we get a so-called 'blocking structure', that is, the

two endpoints of the perimeter edge cannot be connected directly by a spanning tree. Since we already excluded diagonals within the semiar, the vertex neighbouring this perimeter edge also has to be matched by a diagonal in  $M'$ . This vertex exists since we assumed that the size of the semiar is at least 3. We again consider the other endpoint of this even perimeter edge and either construct a boundary area with at least three points (cf. Figure 2.16 (d)), which again leads to a contradiction. Otherwise we get a second blocking structure (cf. Figure 2.16 (e)). However, this concludes this case as well, since the points in between the two blocking structures are separated from the other points and cannot be connected with them by any spanning tree.

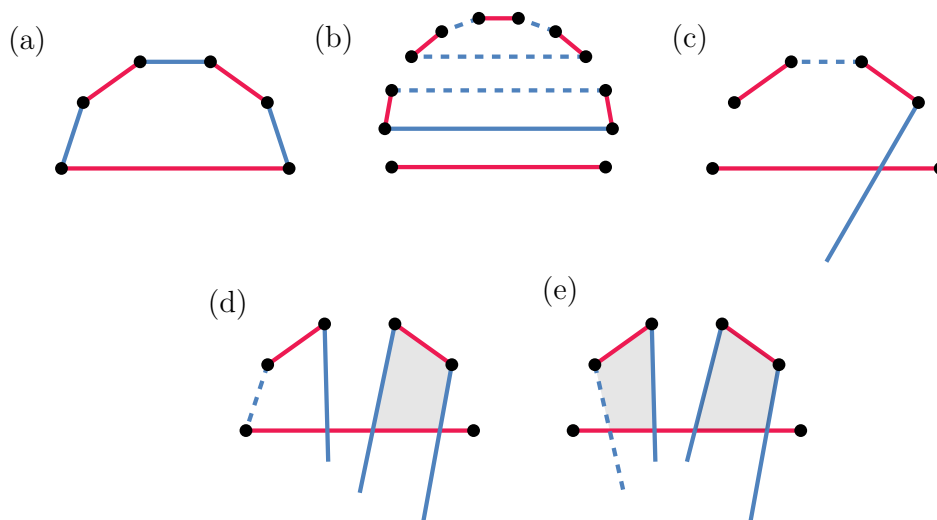


Figure 2.16: All possible cases for a semiar of size  $k \geq 3$  in a matching  $M$  (depicted in red) and a second matching  $M'$  (depicted in blue) which does not use any of the perimeter edges in  $M$ .

It follows that at least one of the perimeter edges in the semiar of  $M$  also lies in  $M'$ . Analogously we can apply the argument for the other semiar.

Case 2: All but one semiear in  $M$  is of size 2

For simplicity we assume w.l.o.g. that there exists an even 2-semiear in  $M$ . Matching the points of this semiear by odd perimeter edges yields an ear, a contradiction by Lemma 2.14 (cf. Figure 2.17 (a)). If one of the endpoints of the even perimeter edge is matched by an odd perimeter edge in  $M'$  and the other one is matched by a diagonal, we get a boundary area with three points, contradicting Lemma 2.14 (cf. Figure 2.17 (b)). Otherwise, both endpoints of the even perimeter edge are matched by diagonals intersecting the diagonal of the 2-semiear (cf. Figure 2.17 (c)). As in the proof of Theorem 2.17 we get a blocking structure, which means that the two endpoints of the perimeter edge cannot be connected directly by a spanning tree. We can assume that this holds for all semiears of size two in  $M$ , otherwise we apply one of the arguments above.

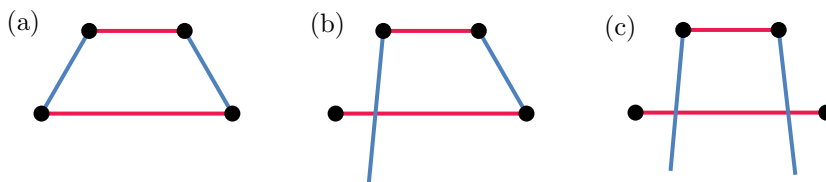


Figure 2.17: All possible cases for a 2-semiear in a matching  $M$  (depicted in red) and a second matching  $M'$  (depicted in blue) which does not use the perimeter edges in  $M$ .

Out of those 2-semiears we choose the one with no further semiear of  $M$  (also not the one of larger size) on one side of a diagonal  $d$  in  $M'$ . This is possible since the number of semiears is finite and the diagonals in  $M'$  cannot intersect each other, therefore there is an ordering of the 2-semiears in  $M$  (and only one semiear of larger size). It is easy to see that the diagonal  $d$  induces a semiear in  $M'$  on this side of the graph. If this semiear is of size 2 and two diagonals in  $M$  are intersecting the diagonal of the semiear, we get another blocking structure. (Otherwise we can apply one of the other arguments above to the semiear in  $M'$  and again end up with a perimeter edge lying in both matchings.) It follows

that both diagonals in  $M$  have to intersect the diagonals in  $M'$  (those which also intersect the even 2-semiear), otherwise we induce another semiear in  $M$  on this side, a contradiction. However, this separates at least three points from the rest and it is not possible to find a common compatible spanning tree (cf. Figure 2.18).

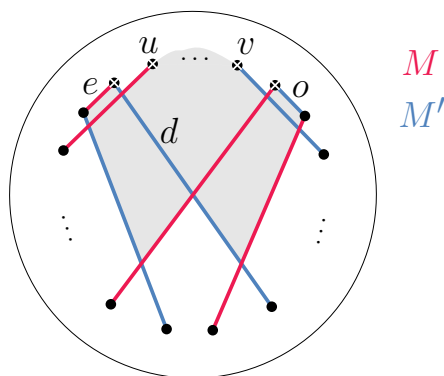


Figure 2.18: An even 2-semiear in  $M$  (red matching edges) intersected by two diagonals in  $M'$  (blue edges) (on the left) and an odd 2-semiear in  $M'$  intersected by two diagonals in  $M$  (on the right). The vertices  $u$  and  $v$  might coincide. The grey areas are blocked, that is, the spanning tree cannot pass them. Therefore, at least three points (if  $u = v$ ) are not reachable from the rest of the vertices (marked by white crosses).

Case 3: All semiears in  $M$  are of size 2

This case works similar to the second case. If the cases (a) or (b) in Figure 2.17 can be applied to two 2-semiears, we are done since both perimeter edges also lie in  $M'$ . If we can apply one of those cases to at least one 2-semiear, we treat this semiear like the semiear of larger size in Case 2 and proceed as before.

Otherwise, all 2-semiears, thus all semiears in  $M$  are as depicted in Figure 2.17 (c). Again there is an ordering of those 2-semiears and now we can choose two of them such that there is no further semiear of  $M$  on one side of a diagonal in  $M'$ . (In one case there is no further semiear on the 'left' side, in the other case there is no semiear on the 'right' side.) It follows that two distinct semiears in  $M'$  are induced. The arguments in

Case 2 can be applied separately to both of them, therefore we end up with at least two perimeter edges which lie in both  $M$  and  $M'$ .

□

**Corollary 2.18.** Let  $S$  be of size  $2n \geq 10$ . For even  $n$ , the distance between an even 2-semiar matching and an odd 2-semiar matching is at least 4. For odd  $n$ , let  $M$  be a near-2-semiar matching with a single odd perimeter edge and  $M'$  be a near-2-semiar matching with a single even perimeter edge such that those two edges are incident in  $S$ . Then the distance between  $M$  and  $M'$  is at least 4.

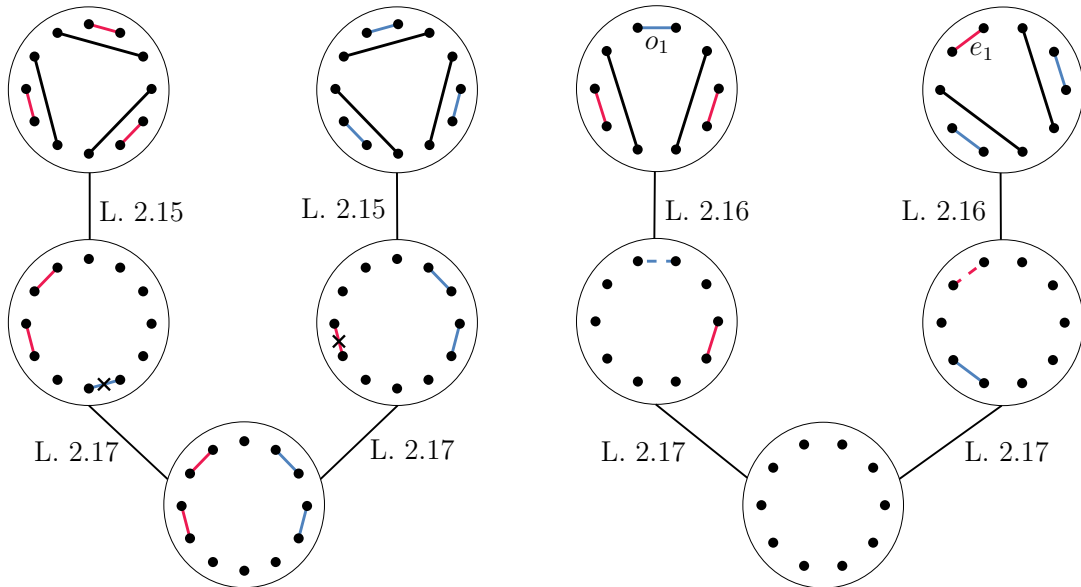


Figure 2.19: Illustrations, that the distance between two special 2-semiar matchings (left) and between two special near-2-semiar matchings (right) is at least 4. Even perimeter edges are drawn in red, odd ones are drawn in blue. The numbers next to the edges indicate which Lemma is applied. Crossed out edges indicate that this type of edge (even or odd) cannot appear in that matching.

*Proof.*

$n$  is even:

By Lemma 2.15 we know that for every matching disjoint tree-compatible to an even 2-semiear matching all perimeter edges are even. Now by Theorem 2.17 all matchings which are disjoint tree-compatible to them contain at least two of their even perimeter edges.

Analogously, in every matching disjoint tree-compatible to an odd 2-semiear matching all perimeter edges are odd, and all matchings disjoint tree-compatible to those contain at least two odd perimeter edges (in particular any matching with no odd perimeter edge is not disjoint tree-compatible).

Combining these results shows that there are at least three intermediate matchings between an even and an odd 2-semiear matching in the disjoint tree-compatible graph.

$n$  is odd:

By Lemma 2.16 every matching disjoint tree-compatible to  $M$  contains at most one odd perimeter edge, namely the same as in  $M$ , say  $o_1$ . Analogously, every matching disjoint tree-compatible to  $M'$  contains no even perimeter edge other than the one in  $M'$ , say  $e_1$ .

As before we can apply Lemma 2.17 and deduce that all matchings disjoint tree-compatible to those with at most one odd or even perimeter edge, respectively, contain at least two perimeter edges. However, since  $o_1$  and  $e_1$  are incident, they cannot both appear in any of the disjoint tree-compatible matchings at the same time, thus the two sets of all disjoint tree-compatible matchings is disjoint which implies a total lower bound of four for the distance of  $M$  and  $M'$ .  $\square$

**Remark 2.19.** The Corollary above states that  $G_{2n}$  is lower bounded by 4. Now it seems reasonable to consider more restricted graph classes and check whether the disjoint compatibility graph is still connected. It is easy to observe that we cannot exclude those graphs containing a path of size  $\Theta(n)$  (all paths are obviously of size  $\mathcal{O}(n)$  since there are exactly  $2n$  vertices): Consider a matching on  $S$  consisting of only parallel matching edges. Starting at one of the two perimeter edges, one can obtain a path in any disjoint compatible spanning tree going from one diagonal to the next one until we reach the other

perimeter edge. This is since the diagonals split the inside of the convex hull in adjacent faces and we cannot cross them and skip any face along the path. Since there is a linear number of faces, the path is of linear size in  $n$  as well.

# 3 Disjoint path-compatible matchings

Research on this topic was initiated during the 16th European Geometric Graph-Week 2020 held near Strobl, Austria [4].

## 3.1 Basic definitions and special cases

Again we consider only graphs, more precisely plane perfect matchings and Hamiltonian paths, which are disjoint to each other. This is because the Hamiltonian path along the perimeter is compatible to all perfect matchings and all other paths. Therefore the case for not necessarily disjoint compatible matchings and paths is rather trivial.

For disjoint path-compatibility, instead of the disjoint path-compatibility graph with all plane perfect matchings as vertices, we consider the bipartite graph  $B_{2n}$  where all plane perfect matchings together with all Hamiltonian paths on a point set  $S$  form the set of vertices. We do so since the matchings are far less connected in this setting and we are rather interested if there even exist disjoint compatible paths and if yes, how many of them.

**Definition 3.1.** The bipartite graph  $B_{2n}$  is defined as follows:

- the two independent and disjoint partitions of vertices are made up of all possible plane perfect matchings and all possible Hamiltonian paths on  $S$ , respectively



- two vertices (on different sides of the partition) are connected by an edge if and only if the respective matching and the respective path are disjoint compatible.

First, we want to find and characterize potentially isolated matchings in  $B_{2n}$ . Therefore we recall how semicycles and semiears were defined in 2.10.

**Definition 2.10.** Let  $M$  be a matching on  $S$ . A  $k$ -semicycle  $X$  is called an *inside  $k$ -semicycle* (or just an *inside semicycle*) if  $\bar{X}$  contains at least two diagonals, otherwise it is called a  *$k$ -semiear* (or just a *semiear*).

**Lemma 3.2.** Let  $M$  be a plane perfect matching on  $S$  with at least three semiears. Then there is no Hamiltonian path on  $S$  which is disjoint compatible to  $M$ , that is,  $M$  is an isolated vertex in  $B_{2n}$ .

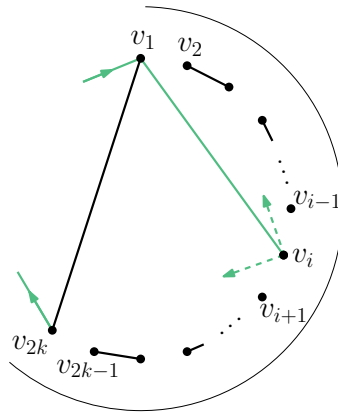


Figure 3.1: A  $k$ -semiear in a plane perfect matching with a possibly disjoint compatible path drawn in green entering the ear at  $v_1$  and leaving it at  $v_{2k}$ . If the path reaches vertex  $v_i$ , it can only traverse vertices with index either smaller or larger than  $i$  afterwards.

*Proof.* We claim that any semiear in a matching  $M$  has to contain an end of a disjoint compatible path. By contradiction, we assume the contrary. We

consider a  $k$ -semiar and label the  $2k$  vertices of the semiar along the boundary of the convex hull by  $v_i$ , that is, the path enters the semiar at vertex  $v_1$  and leaves it at  $v_{2k}$ .

Observe that once the path reaches vertex  $v_i$ , it can only visit either vertices with smaller or larger index (cf. Figure 3.1). Therefore we need to go along them in ascending order. However this is not possible since we demand disjoint compatibility. This proves that in every semiar of  $M$  any disjoint compatible path has to start or end there, thus no matching with three or more semiar contains such a path.  $\square$

Now we consider plane perfect matchings with exactly one semiar, i.e., perimeter matchings, and show that they have exponentially many disjoint compatible paths.

**Lemma 3.3.** Let  $M$  be a perimeter matching on a set  $S$  of  $2n$  points. Then there are  $\frac{n}{3}(2^{n-1} + (-1)^n)$  plane Hamiltonian paths which are disjoint compatible to  $M$ .

*Proof.* First, we pick a fixed starting point  $p$  and denote by  $f(n)$  the number of paths which are disjoint compatible to  $M$  and start in  $p$ . For the second and third vertex along the path, there is only one possibility to chose if we want to cover all  $2n$  points.

Therefore we consider all possibilities for our path to go along until we hit a further yet unvisited matching edge to deduce a recursion. There are in total three possible ways to do so, depicted in Figure 3.2. For the first case, moving along corresponds to a disjoint compatible path on  $n - 1$  perimeter matching edges and for the other two cases the second part of the path corresponds to a disjoint compatible path on  $n - 2$  perimeter matching edges. This equivalence is depicted in the bottom row of Figure 3.2.

The latter two path starts only work for at least four matching edges, thus for  $n \geq 4$  we obtain the recursive formula  $f(n) = f(n - 1) + 2f(n - 2)$  on the

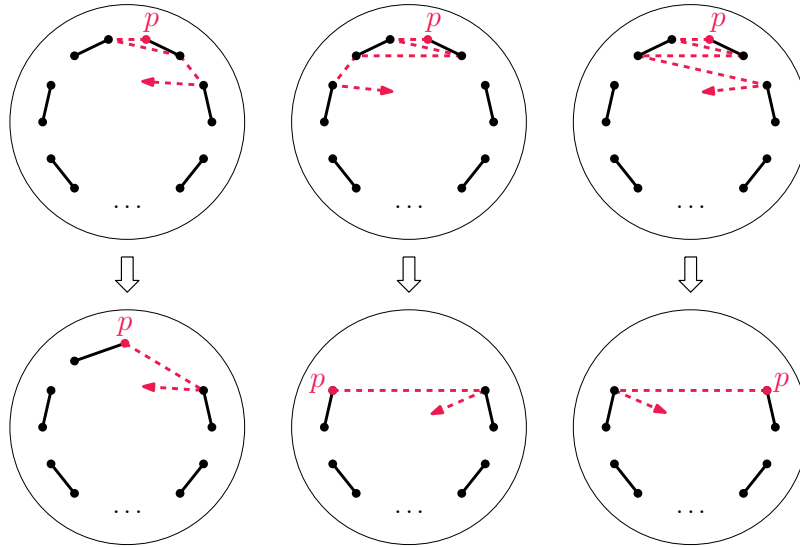


Figure 3.2: For a fixed point  $p$  there are three possible starts for a path on  $n$  perimeter matching edges (top row). They can recursively be continued on sets with  $n - 1$ ,  $n - 2$ , and again  $n - 2$  matching edges, respectively.

number of disjoint compatible paths for  $2n$  matching edges starting in  $p$ . For two or three matching edges, only the first starting case is possible. Therefore, there is only one such disjoint compatible path. For one single matching edge, no such path exists. This yields the recursion start  $f(1) = 0$ ,  $f(2) = f(3) = 1$ .

Solving this recurrence, which is known as Jacobsthal sequence (cf. [10]) with an index shift by one, we obtain  $f(n) = \frac{2^{n-1} + (-1)^n}{3}$ . Our starting point  $p$  was chosen arbitrarily out of  $2n$  points, we however do not distinguish between starting and ending points. Therefore we need to multiply the result by  $\frac{2n}{2}$  which eventually yields the result  $\frac{n}{3}(2^{n-1} + (-1)^n)$  for  $n \geq 1$ .  $\square$

We covered all plane perfect matchings with either one or at least three semiears. Therefore, the only matchings left are those with exactly two semiears. This case is by far the most comprehensive one.

### 3.2 Plane perfect matchings with two semiears

To analyse matchings with exactly two semiears, we introduce the notion of  $(k, l)$ -faces.

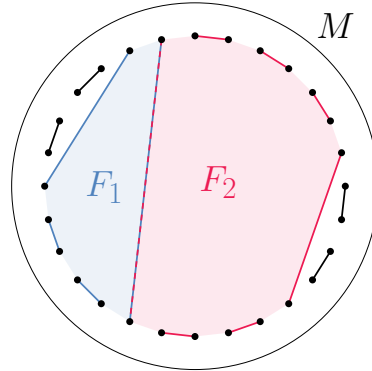


Figure 3.3: A plane perfect matching  $M$  on  $S$  with two semiears, two faces and their convex hulls. A  $(0, 2)$ -face  $F_1$  is drawn in blue and a  $(2, 3)$ -face  $F_2$  is depicted in red.

**Definition 3.4.** Let  $M$  be a plane perfect matching on  $S$  with two semiears. We define a  $(k, l)$ -face for  $0 \leq k \leq l$  to be an inside  $(k + l + 2)$ -semicycle with exactly two diagonals,  $k$  perimeter edges on one side of the convex hull and  $l$  perimeter edges on the other side.

**Remark 3.5.**  $(k, l)$ -faces could also be defined for general plane perfect matchings on  $S$ , however this is not needed here.

We observe that every plane perfect matching with two semiears consists of a chain of faces, starting and ending with a semiear. The diagonals are used twice, respectively, and separate either two faces or a face and a semiear. Note, however, that the number of faces could be zero.

Any Hamiltonian path which is disjoint compatible to a matching with two semiears has to traverse this chain of faces from one end to the other, starting

and ending in a semiear, respectively. We therefore can check for any plane perfect matching of this type by scanning from left to right if there exists such a path.

When traversing from one face to another (or from/to a semiear), the path crosses at one endpoint of the respective diagonal. The other point incident to this diagonal has to be visited either before (in the first face/semiear) or afterwards (in the second face/semiear). This yields in total four different possibilities for any diagonal as shown in Figure 3.4.

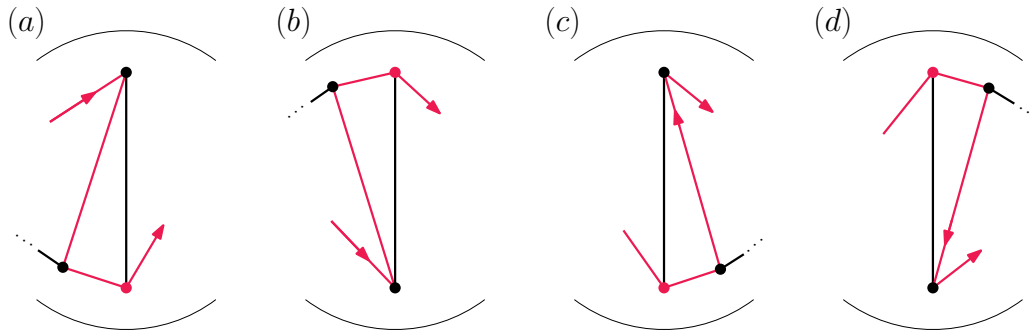


Figure 3.4: The four different ways of a path visiting the two endpoints of a diagonal, here drawn in black. In the two figures on the left, the path meets one of the points before crossing to the second face, that is, within the first face. In the two figures on the right, the path first traverses to the second face and only afterwards visits the second incident point of the diagonal.

Our next step is to consider which faces locally admit a disjoint compatible path and if they do, how many different of these paths are there. We are furthermore interested in the possible ways of processing the diagonals of the respective face. First of all, for too 'unbalanced' faces, i.e.,  $(k, l)$ -faces with  $k$  and  $l$  being far off, there is no disjoint compatible Hamiltonian path.

**Lemma 3.6.** Any  $(k, l)$ -face with  $l \geq 2k + 3$  does not admit a disjoint compatible Hamiltonian path. In particular, every plane perfect matching on  $S$  with two semiears and such a face is isolated in the bipartite graph  $B_{2n}$ .

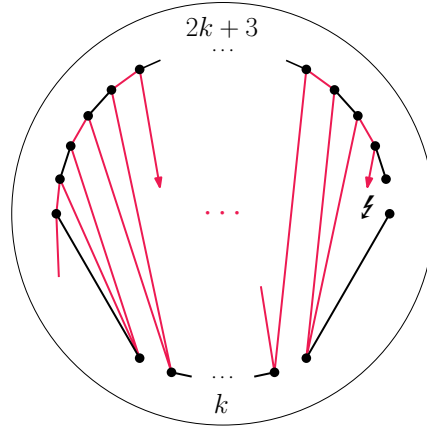


Figure 3.5: There is no disjoint compatible Hamiltonian path meeting all points of a  $(k, 2k + 3)$ -face: even if we try to visit as many point on the upper arc of the convex hull as possible, the path (drawn in red) misses at least two points and therefore cannot leave the face.

*Proof.* We will show that in a  $(k, 2k + 3)$ -face, not all  $2k + 3$  edges on the larger side of the face can be visited by a disjoint compatible path. This implies our statement also for all  $(k, l)$ -faces with  $l$  even larger.

First, we observe that any path has to switch between the two sides of the face (for simplicity, we refer here to the larger side with  $2k + 3$  edges by *above* and to the  $k$  edges on the other side by *below*). After passing at most two points on one side (not adjacent by a matching edge), we have to go to the other side. Above there are in total  $4k + 8$  points to visit (including those incident to the diagonals) and below there are  $2k + 2$  points overall.

If we want to saturate as many points above as possible, it is easy to see that we have to apply option (d) as depicted in Figure 3.4 for the first diagonal and option (b) for the second diagonal (when going from left to right). By doing so, we can visit the first two points above without using any of the points below, and afterwards for every point below we can meet two further points above. However, after we passed all  $2k + 2$  points below, the path visited only  $4k + 6$  points above and cannot reach the last two points above to leave the face.  $\square$

**Corollary 3.7.** Any  $(k, 2k + 2)$ -face with  $k \geq 0$  admits a unique disjoint compatible Hamiltonian path. In particular, the way how the two respective diagonals are visited is fixed.

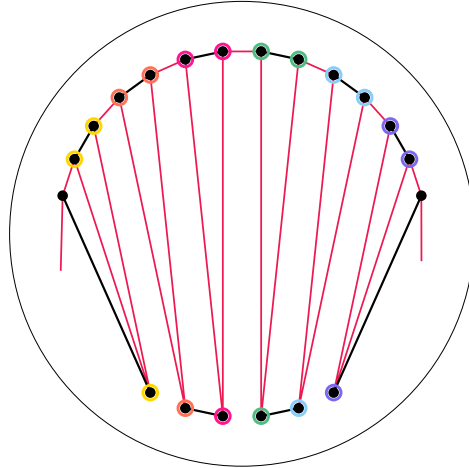


Figure 3.6: A  $(2, 6)$ -face as an example for a  $(k, 2k + 2)$ -face with a unique disjoint compatible Hamiltonian path drawn in red. The circles indicate which point on the smaller side with  $2k + 2 = 6$  points saturates which two points on the larger side. The leftmost and rightmost points are those where the path is entering and leaving the face, respectively.

*Proof.* The statement immediately follows from the proof of Lemma 3.6 where a Hamiltonian path was constructed such that it visits as many points on the larger side of the face as possible. This path is unique and visits exactly  $4k + 6$  points on one side and  $2k + 2$  points on the other side as required.  $\square$

**Lemma 3.8.** For any  $(k, 2k + 1)$ -face with  $k \geq 0$  there are three different possibilities for a disjoint compatible Hamiltonian path w.r.t. the interaction of the path with the two diagonals (up to symmetry).

*Proof.* To find all possibilities we again consider a  $(k, 2k + 2)$ -face as in Corollary 3.7 which admits one unique disjoint compatible Hamiltonian path. Every

point on the smaller side satisfies exactly two points on the larger side and the path has to enter and leave at the larger side.

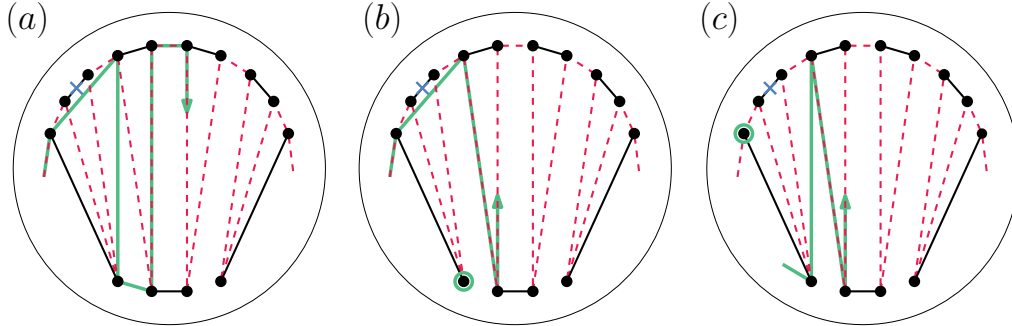


Figure 3.7: A  $(k, 2k + 2)$ -face with its unique disjoint compatible Hamiltonian path depicted in red (dashed). Deleting one matching edge on the upper arc (crossed in blue) yields a  $(k, 2k + 1)$ -face. There are three different ways for a disjoint compatible Hamiltonian path to run in this face as depicted in green. The points encircled in green are visited by the path outside of the face.

If we now remove one matching edge, that is, two points on the larger side, there are several possibilities. One way is to interact with the diagonals in the same way and two vertices below only saturating one point above, respectively, as seen in Figure 3.7 (a). Another way is to enter and leave the face again on the larger side, but leave out one of the lower points incident to the diagonal and meet it outside the face, cf. Figure 3.7 (b). Then the path has to continue as for the  $(k, 2k + 2)$ -face. The third option is to enter (or leave) the face at one diagonal on the smaller side. In that case, the adjacent point on this diagonal has to be left out, otherwise it is not possible to meet all inner points of the face. The rest of the face is processed again as in the  $(k, 2k + 2)$ -face, cf. Figure 3.7 (c).  $\square$

Combining the preceding results we can now obtain an algorithm to decide whether there is a disjoint compatible Hamiltonian path for a given plane perfect matching on  $S$  with exactly two ears.

As we already observed earlier, each such matching forms a chain, starting



with a semiear, followed by (possibly zero)  $(k, l)$ -faces and ending with another semiear. The idea is to pass through this chain with a scanline going from diagonal to diagonal. There are four possibilities for each diagonal to be traversed by a disjoint compatible path as depicted in Figure 3.4.

We start with one semiear and identify the disjoint compatible Hamiltonian paths for it. Here, two paths are considered to be different if the diagonal is processed differently, therefore there are at most four possible options. As shown in Figure 3.8 it is easy to see that there are two feasible paths for a 2-semiear, namely options (a) and (b) in Figure 3.4 for the ear "on the left" (which is treated first) and options (c) and (d) for the ear "on the right" (visited at the end of the algorithm). For any  $k$ -semiear with  $k \geq 3$  all four options are valid.

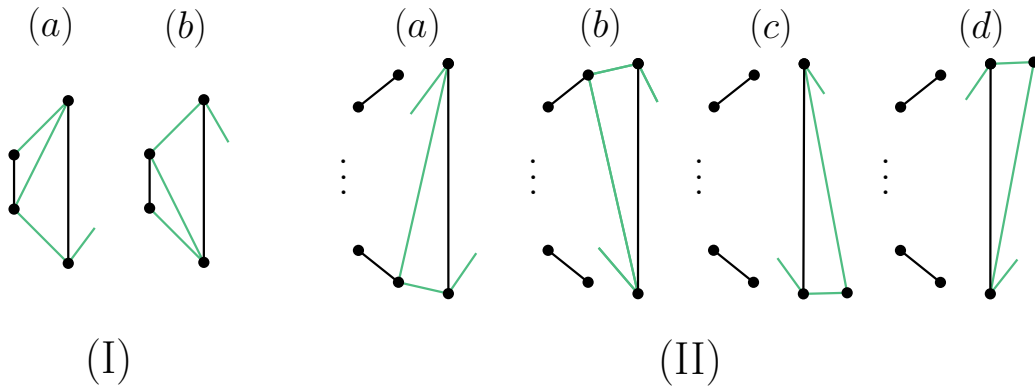


Figure 3.8: (I) Two different disjoint compatible paths for a 2-semiear. They meet both endpoints of the diagonal within the semiear and leave either above or below. (II) For a semiear with at least three perimeter edges, any variant of a disjoint compatible path is feasible.

Now at each diagonal crossover following a  $(k, l)$ -face, we identify the possible ways for a Hamiltonian path to pass, given as input the feasible paths of the previous diagonal. Therefore we have to check the size of the respective face, more precisely, the parameters  $k$  and  $l$ . (W.l.o.g. we assume that  $0 \leq k \leq l$ , where  $k$  is the number of matching edges below and  $l$  is the number of matching edges above. Otherwise we just need to reflect the interaction possibilities of a path with the diagonal across the horizontal axis, that is, exchange the role

of (a), (b) and (c), (d), respectively.) We distinguish between the following cases:

- $l \geq 2k + 3$ : Regardless of the input, the set of feasible paths as output is empty. This case is treated in **Lemma 3.6**.
- $l = 2k + 2$ : If possibility (d) is part of the input, the output contains possibility (b). Otherwise, the output is empty. This case is treated in **Corollary 3.7**.
- $l = 2k + 1$ : If the input contains possibilities (a) or (b), we get (b) as feasible option in the output. For input (d), the output contains (b), (c) and (d). If the input consists of only (c) or is empty, then the output set is also empty. This case is covered by **Lemma 3.8** considering symmetry.

- $l = 2k, k \geq 1$ : Similar to the above cases we obtain the following implications by checking all combinations: If  $(c)$  is a feasible input,  $(b)$  is in the output. If  $(a)$  or  $(b)$  are part of the input, the output contains  $(b)$ ,  $(c)$  and  $(d)$ . Input  $(d)$  implies that all four possibilities are feasible. A proof by picture is given in **Figure 3.9**.

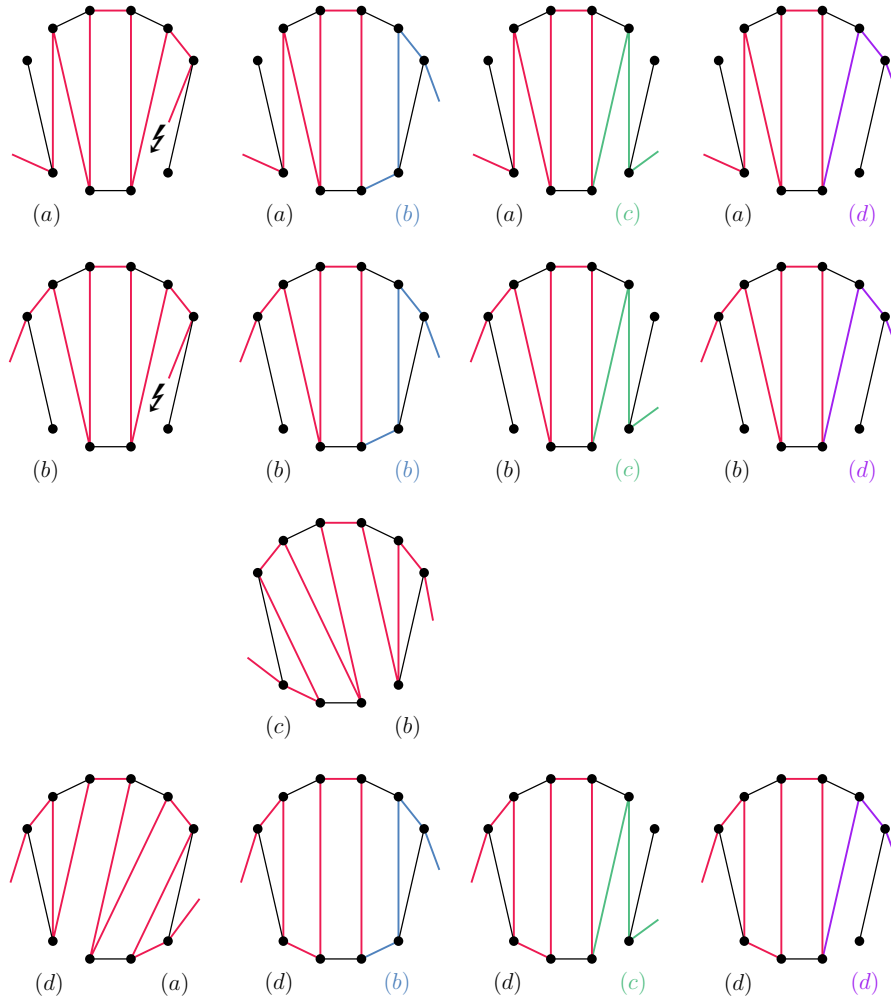


Figure 3.9: All possible kinds of disjoint compatible paths in a  $(k, 2k)$ -face, depicted for  $k = 1$ .

- $l = 2k - 1, k \geq 1$ : If the input contains (c), then (b), (c) and (d) are in the output set. If any other option is in the input, again all possibilities are feasible. A proof by picture is given in **Figure 3.10**.  
(Note: This case includes (1, 1)-faces.)

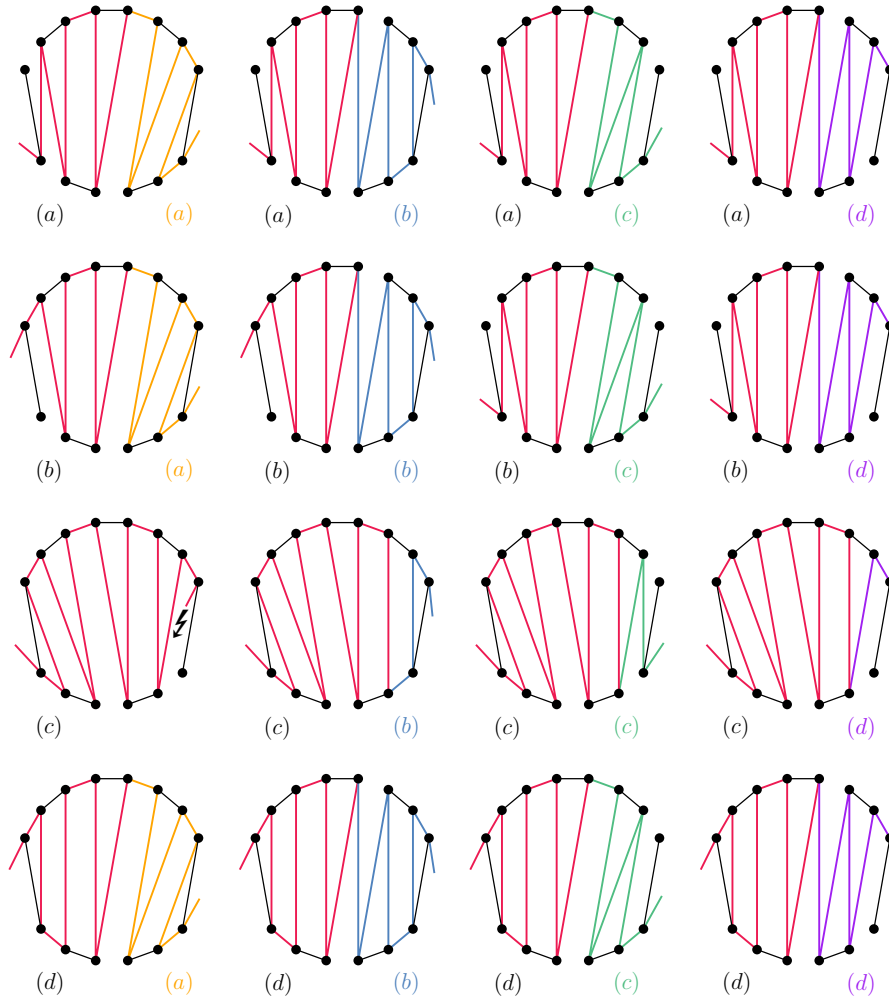


Figure 3.10: All possible kinds of disjoint compatible paths in a  $(k, 2k - 1)$ -face, depicted for  $k = 2$ .

- $2 \leq k \leq l \leq 2k - 2$ : As long as the input is not empty, the output contains all four possibilities. Those are depicted for the extreme case  $l = 2k - 2$  in **Figure 3.11**.

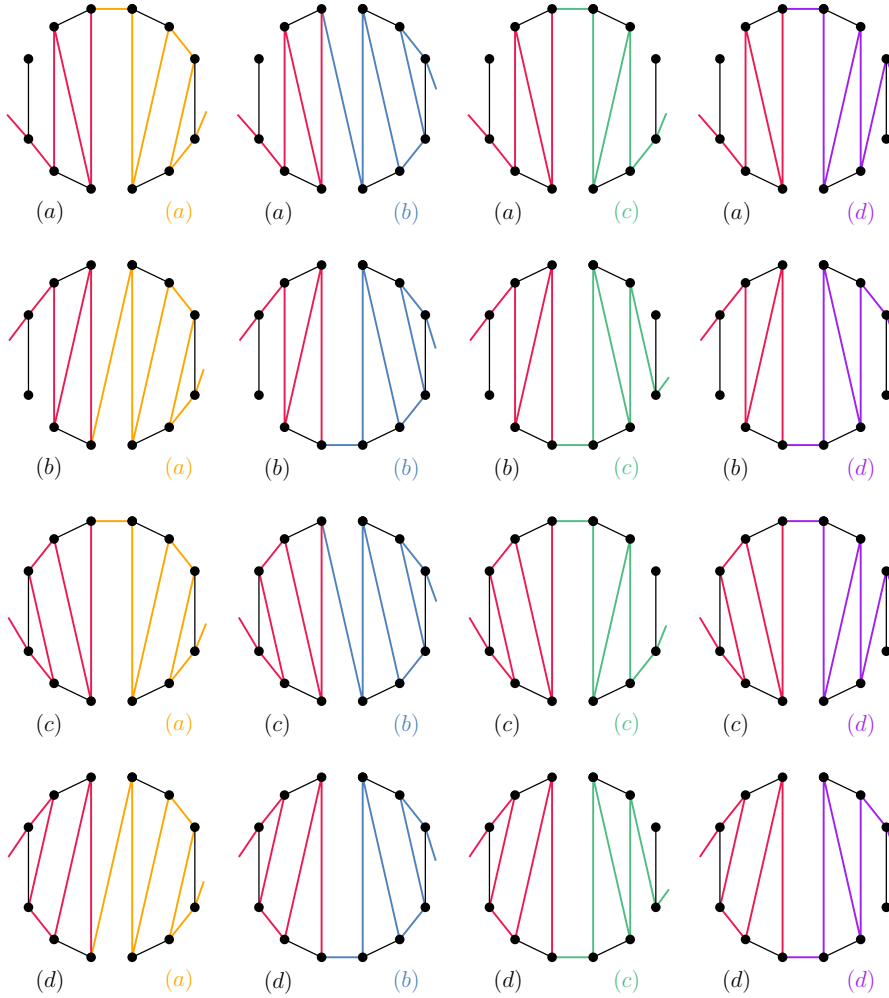


Figure 3.11: All possible kinds of disjoint compatible paths in a  $(k, l)$ -face for  $2 \leq k \leq l \leq 2k - 2$ , depicted for  $k = l = 2$ .

- $l = 0, k = 0$ : If the input contains (a) or (b), it follows that (c) and (d) are in the output set. If the input contains (c), then (b) is a feasible output and (d) in the input set implies that (a) is a valid possibility for the output. A proof by picture is given in **Figure 3.12**.

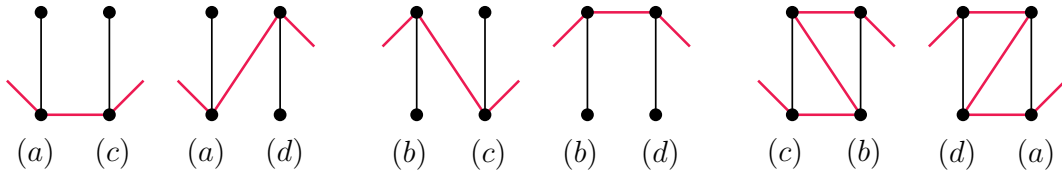


Figure 3.12: All possible kinds of disjoint compatible paths in a  $(0,0)$ -face.

An overview of all different output cases is depicted in Table 3.1.

case	input			
	(a)	(b)	(c)	(d)
$l \geq 2k + 3$	$\emptyset$	$\emptyset$	$\emptyset$	$\emptyset$
$l = 2k + 2$	$\emptyset$	$\emptyset$	$\emptyset$	(b)
$l = 2k + 1$	(b)	(b)	$\emptyset$	(b),(c),(d)
$l = 2k, k \geq 1$	(b),(c),(d)	(b),(c),(d)	(b)	(a),(b),(c),(d)
$l = 2k - 1, k \geq 1$	(a),(b),(c),(d)	(a),(b),(c),(d)	(b),(c),(d)	(a),(b),(c),(d)
$2 \leq k \leq l \leq 2k - 2$	(a),(b),(c),(d)	(a),(b),(c),(d)	(a),(b),(c),(d)	(a),(b),(c),(d)
$l = k = 0$	(c),(d)	(c),(d)	(b)	(a)

Table 3.1: All valid output cases of the algorithm for a given  $(k,l)$ -face with the respective input case. If the input contains several cases, then the output is the union of the corresponding entries in the table.

For a matching on  $2n$  points (with two semiears), there are at most  $n - 3$  faces. Each of them, as well as the semiears, can be treated in constant time. Therefore the running time for the algorithm is of order  $\mathcal{O}(n)$ .

Figure 3.13 gives an example of how the algorithm works.

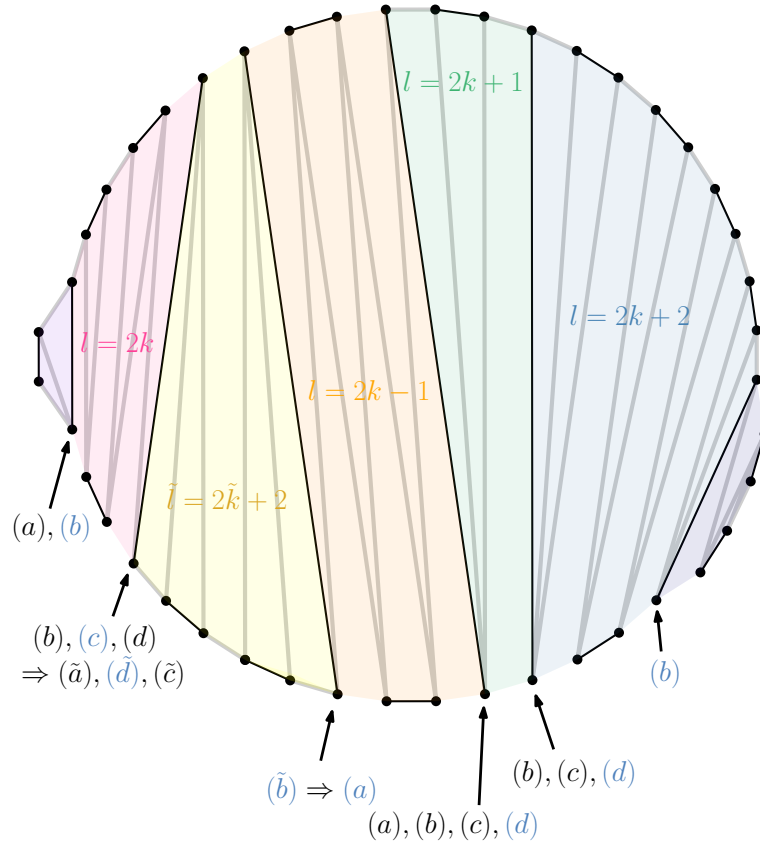


Figure 3.13: A plane perfect matching with two semiarcs on a set of 44 points in convex position. The semiarcs and faces are depicted in different colours. For each diagonal, it is indicated which options for a disjoint compatible Hamiltonian path are feasible. All values provided with a tilde refer to the reflection of the respective face across the horizontal axis. The set of feasible interactions of a path with the diagonals is not empty at any point. For a 3-semiarc as in this example on the right, any option is valid. Therefore a (not necessarily unique) disjoint compatible Hamiltonian path exists; one of them is indicated in grey and the respective options chosen at the diagonals are highlighted in blue. If the semiarc on the right was a 2-semiarc, then no disjoint compatible path would exist since this would require either option (c) or (d) for the rightmost diagonal.

**Lemma 3.9.** Any plane perfect matching consisting of an odd number of parallel matching edges (that is, only  $(0, 0)$ -faces and two 2-ears) obtains no disjoint compatible Hamiltonian path, i.e., those matchings are isolated vertices in  $B_{2n}$ .

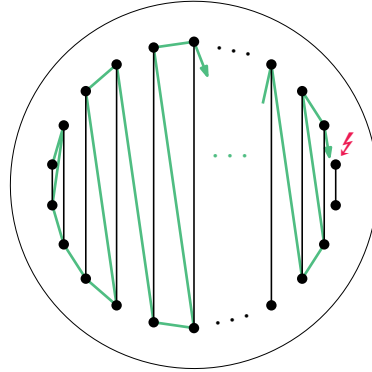


Figure 3.14: A plane perfect matching consisting of an odd number of parallel matching edges. The faces have to be treated alternately, therefore a parity conflict arises and there is no possibility to draw a disjoint compatible Hamiltonian path.

*Proof.* For both ears, the path has to visit both endpoints of the diagonal within this ear to reach both points of the perimeter edge. For a  $(0, 0)$ -face, there are two possibilities. Either the path visits all four points within the face or only two of them, one of each diagonal.

Since the path meets both points of the first diagonal within the ear, it only meets two in the adjacent first face. This again implies that it has to saturate all four points in the second face, therefore the path only meets two vertices in the third face, etc. If we number the faces (but not the ears) from left to right, we observe that within all faces of odd index, two vertices are visited and within all faces of even index, four vertices are visited. However, we have an even number of  $(0, 0)$ -faces, thus in the last of those faces, which is adjacent to the second 2-ear, all four vertices are met and it is impossible to reach both points incident to the second perimeter edge.  $\square$



**Definition 3.10.** Let  $M, M'$  be two plane perfect matchings on  $S$ . If there exists a plane Hamiltonian path  $P$  on  $S$  such that both  $M$  and  $M'$  are disjoint compatible to  $P$ , then  $M$  and  $M'$  are called *disjoint path-compatible*.

We recall a Lemma about disjoint tree-compatible matchings:

**Lemma 2.14.** Let  $M, M'$  be two matchings whose symmetric difference is an ear or a boundary area with at least three points. Then  $M$  and  $M'$  are not disjoint tree-compatible to each other.

By this statement we can easily conclude the following statement about disjoint path-compatible matchings:

**Lemma 3.11.** Let  $M$  and  $M'$  be two matchings whose symmetric difference is an ear or a boundary area. Then  $M$  and  $M'$  are not disjoint path-compatible to each other.

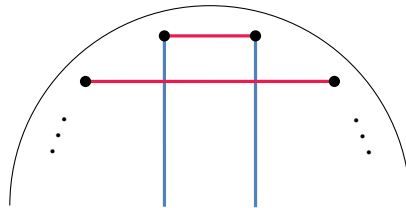


Figure 3.15: Two matchings creating a boundary area with two points.

*Proof.* Every path is a tree, therefore the only case left to consider is a pair of matchings creating a boundary area with two points. This situation is depicted in Figure 3.15. The red matching creates a 2-semiear, thus has at least one further semiear. However, the only way for a disjoint compatible Hamiltonian path to visit the two upper points is to start and end at those points, respectively. This is a contradiction to the fact that every semiear has to contain the start or end of any disjoint compatible path.  $\square$

### 3 Disjoint path-compatible matchings

---

Unlike for disjoint tree-compatible matchings, the set of all plane perfect matchings on  $S$  is not connected w.r.t. disjoint path-compatibility for sufficiently large  $n$  as the values in Table 3.2 suggest, even when restricting to only non-isolated matchings in  $B_{2n}$ . This statement can be proven by considering the two perimeter matchings.

$2n$	number of matchings	number of paths	components with matchings	number of isolated paths
4	2	8	2 components in total: <ul style="list-style-type: none"> <li>• 2x: 1 matching, 2 paths</li> </ul>	4
6	5	48	5 components in total: <ul style="list-style-type: none"> <li>• 2x: 1 matching, 3 paths</li> <li>• 3x: 1 matching, 0 paths</li> </ul>	42
8	14	256	10 components in total: <ul style="list-style-type: none"> <li>• 2x: 3 matchings, 16 paths</li> <li>• 8x: 1 matching, 4 paths</li> </ul>	192
10	42	1280	27 components in total: <ul style="list-style-type: none"> <li>• 2x: 6 matchings, 35 paths</li> <li>• 5x: 2 matchings, 6 paths</li> <li>• 5x: 1 matching, 8 paths</li> <li>• 15x: 1 matching, 0 paths</li> </ul>	1140
12	132	6144	54 components in total: <ul style="list-style-type: none"> <li>• 2x: 16 matchings, 156 paths</li> <li>• 12x: 5 matchings, 34 paths</li> <li>• 24x: 1 matching, 4 paths</li> <li>• 16x: 1 matching, 0 paths</li> </ul>	5328

### 3 Disjoint path-compatible matchings

---

14	429	28672	219 components in total: <ul style="list-style-type: none"> <li>• 2x: 36 matchings, 406 paths</li> <li>• 7x: 11 matchings, 70 paths</li> <li>• 7x: 7 matchings, 86 paths</li> <li>• 14x: 3 matchings, 8 paths</li> <li>• 14x: 1 matching, 12 paths</li> <li>• 175x: 1 matching, 0 paths</li> </ul>	26488
16	1430	131072	678 components in total: <ul style="list-style-type: none"> <li>• 2x: 97 matchings, 1504 paths</li> <li>• 16x: 24 matchings, 288 paths</li> <li>• 32x: 7 matchings, 54 paths</li> <li>• 96x: 1 matching, 4 paths</li> <li>• 532x: 1 matching, 0 paths</li> </ul>	121344
18	4862	589824	2936 components in total: <ul style="list-style-type: none"> <li>• 2x: 217 matchings, 4239 paths</li> <li>• 9x: 60 matchings, 694 paths</li> <li>• 9x: 40 matchings, 810 paths</li> <li>• 18x: 20 matchings, 129 paths</li> <li>• 18x: 9 matchings, 176 paths</li> <li>• 18x: 4 matchings, 8 paths</li> <li>• 72x: 2 matchings, 6 paths</li> <li>• 36x: 1 matching, 6 paths</li> <li>• 36x: 1 matching, 8 paths</li> <li>• 2718x: 1 matching, 0 paths</li> </ul>	560880
20	16796	2621440	10746 components in total: <ul style="list-style-type: none"> <li>• 2x: 556 matchings, 14330 paths</li> <li>• 20x: 123 matchings, 2472 paths</li> <li>• 40x: 40 matchings, 587 paths</li> <li>• 40x: 9 matchings, 72 paths</li> <li>• 20x: 9 matchings, 60 paths</li> <li>• 20x: 7 matchings, 60 paths</li> <li>• 40x: 5 matchings, 34 paths</li> <li>• 40x: 4 matchings, 46 paths</li> </ul>	2509120

### 3 Disjoint path-compatible matchings

---

			<ul style="list-style-type: none"> <li>• 20x: 4 matchings, 9 paths</li> <li>• 20x: 1 matching, 24 paths</li> <li>• 20x: 1 matching, 8 paths</li> <li>• 360x: 1 matching, 4 paths</li> <li>• 10104x: 1 matching, 0 paths</li> </ul>	
22	58786	11534336	43023 components in total: <ul style="list-style-type: none"> <li>• 2x: 1266 matchings, 42064 paths</li> <li>• 11x: 306 matchings, 6440 paths</li> <li>• 11x: 225 matchings, 7280 paths</li> <li>• 22x: 120 matchings, 1525 paths</li> <li>• 22x: 61 matchings, 1953 paths</li> <li>• 22x: 32 matchings, 234 paths</li> <li>• 22x: 32 matchings, 178 paths</li> <li>• 44x: 27 matchings, 271 paths</li> <li>• 22x: 11 matchings, 308 paths</li> <li>• 22x: 11 matchings, 292 paths               <ul style="list-style-type: none"> <li>• 22x: 5 matchings, 8 paths</li> <li>• 88x: 3 matchings, 6 paths</li> <li>• 264x: 2 matchings, 6 paths</li> <li>• 88x: 1 matching, 20 paths</li> <li>• 88x: 1 matching, 12 paths</li> <li>• 132x: 1 matching, 8 paths</li> <li>• 110x: 1 matching, 4 paths</li> </ul> </li> <li>• 42031x: 1 matching, 0 paths</li> </ul>	11181984

Table 3.2: Key values for the bipartite graph  $B_{2n}$  such as the number of matchings and paths in total (which is the number of vertices in  $B_{2n}$ ) as well as the number of components with matchings and isolated paths for  $n = 1, \dots, 11$  obtained by computer calculations.

**Theorem 3.12.** The two perimeter matchings are not connected in  $B_{2n}$ .

*Proof.* Consider the even perimeter matching. It is easy to see that every disjoint path-compatible matching only has semiears with even perimeter edges, otherwise the union of the two matchings would contain an ear, contradicting Lemma 3.11. We call this semiears *even semiears* for short.

Our claim is now that any matching which is disjoint path-compatible to a matching with only even semiears has only even semiears itself. Since we already covered the perimeter matching, we only have to consider matchings with exactly two (even) semiears. By contradiction, assume that there exists a disjoint path-compatible matching with an odd semiear. If the interior of this semiear intersects with the interior of an even semiear in the first matching, this creates either an ear or a boundary area, which is a contradiction. Otherwise, the union of the two matchings has at least three semiears, therefore no disjoint compatible Hamiltonian path can exist.

Thus we can conclude that any matching in the same connected component as the even perimeter matching only has even semiears and analogously any matching in the same component as the odd perimeter matching obtains only odd semiears. Consequently, those sets are disjoint in the graph  $B_{2n}$ .  $\square$

# 4 Disjoint caterpillar-compatible matchings

Research on this topic is based on joint work in [5].

## 4.1 Basic definitions and general case

In the previous chapters, we have seen that the set of all plane perfect matchings on  $S$  is connected via disjoint compatible spanning trees (for  $n$  sufficiently large) but not connected for Hamiltonian paths which are just a special case of spanning trees.

Therefore the natural question arises whether we can do better, that is, restrict spanning trees in a way that the underlying disjoint compatibility graph is still connected. In fact, we will show that all plane perfect matchings on  $S$  for large enough  $n$  are disjoint compatible via caterpillar trees of maximum degree 3.

**Definition 4.1.** A *caterpillar tree* (or *caterpillar* for short) is a tree consisting of a path and vertices directly connected to this path. We refer to the path as the *spine* of the caterpillar and to the edges connecting the leaves of the tree to the path as the *legs* of the caterpillar.

A caterpillar that includes all vertices on the point set  $S$  is called a *spanning caterpillar*.

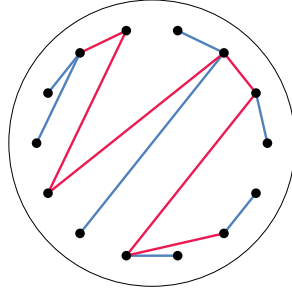


Figure 4.1: A (spanning) caterpillar on a convex set of 14 points. The spine is depicted in red, the legs are drawn in blue.

**Definition 4.2.** Let  $M, M'$  be two plane perfect matchings on  $S$ . If there exists a plane spanning caterpillar  $C$  on  $S$  such that both  $M$  and  $M'$  are disjoint compatible to  $C$ , then  $M$  and  $M'$  are called *disjoint caterpillar-compatible*.

**Definition 4.3.** The *disjoint caterpillar-compatibility graph*  $C_{2n}$  is defined as follows:

- the set of vertices is made up of all possible plane perfect matchings on  $S$
- two vertices are connected by an edge if and only if the respective matchings are disjoint caterpillar-compatible.

The first step is now to show that all plane perfect matchings on  $S$  are indeed connected via disjoint compatible caterpillars.

**Theorem 4.4.** For  $2n \geq 10$ , the disjoint caterpillar-compatibility graph  $C_{2n}$  is connected and  $\text{diam}(C_{2n}) = O(n)$ .

*Proof.* We will make use of the proof of Theorem 2.9. There it was shown that we can get from any plane perfect matching on  $S$  to any other plane perfect matching in at most four steps via matchings differing in only a set of disjoint inside cycles.

For caterpillars, we will show that each of these steps can be done in linearly many steps in the graph  $C_{2n}$ , that is, between two matchings with a symmetric

difference consisting of disjoint inside cycles we can find a sequence of  $O(n)$  disjoint caterpillar-compatible matchings.

In contrast to general spanning trees, the inside cycles are not treated all at once, but one after the other. The number of disjoint inside cycles is at most linear in the size of the point set  $S$ . Therefore it suffices to show that we can rotate one single inside cycle in one step via a disjoint compatible caterpillar.

First, we observe that for any matching edge  $\overline{AB}$  in an arbitrary matching, we can find a disjoint compatible caterpillar going from  $A$  to  $B$  in a greedy way. Starting with the spine at point  $A$ , we always go to the next possible point along the perimeter. If a point is skipped, the next one is reachable for sure and we connect the skipped point by a leg to the newly added point on the spine. By this procedure we get a caterpillar from  $A$  to  $B$  such that the degree of  $A$  is 1, the degree of  $B$  is either 1 or 2 and the maximum degree of the caterpillar is at most 3, cf. Figure 4.2.

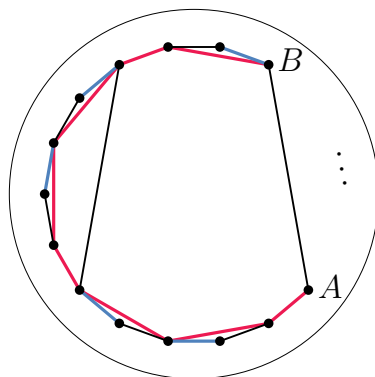


Figure 4.2: A disjoint compatible caterpillar from  $A$  to  $B$  with maximum degree 3. The spine is depicted in red, the legs are drawn in blue.

Now assume that we are given two plane perfect matchings on  $S$  such that their symmetric difference is a single inside cycle. For simplicity we first assume that this cycle contains exactly two diagonals, say  $\overline{A_1B_1}$  and  $\overline{A_2B_2}$  in the sense that  $A_1$  and  $A_2$  are neighbored if we order those four points along the circle as depicted in Figure 4.3. We start by creating a disjoint compatible caterpillar



going from  $A_1$  to  $B_1$ . Then connect all points on the cycle between  $A_1$  and  $A_2$  to  $B_1$  (those edges are legs of the caterpillar) and add an edge between  $B_1$  and  $A_2$  as part of the spine. All points on the cycle between  $B_1$  and  $B_2$  are attached to  $A_2$  via legs again. Finally, create a caterpillar going from  $A_2$  to  $B_2$ .

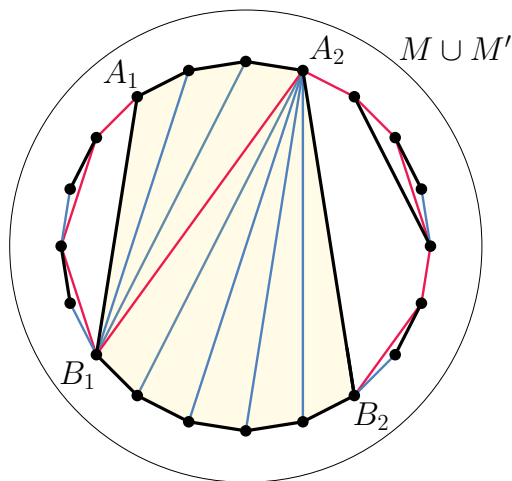


Figure 4.3: Union of two plane perfect matchings  $M$  and  $M'$  drawn in black with a symmetric difference of a single inside cycle containing two diagonals (shaded in gold) and a disjoint compatible caterpillar with red spine and blue legs.

If the inside cycle contains more than two diagonals, say  $\overline{A_1B_1}, \dots, \overline{A_kB_k}$  for  $k \geq 3$ , we can generalise this approach easily: the diagonals are labelled alternately such that the ordering along the inside cycle is in the following way:  $A_1A_2B_2B_3A_3A_4 \dots B_1$ , cf. Figure 4.4. The spine again starts going from  $A_1$  to  $B_1$  as before, then within the cycle reaches  $A_2$ , continues outside the cycle to  $B_2$  and connects  $B_2$  again within the inside cycle to  $A_3$  and so on until we reach  $A_k$  and finally finish the spine by going to  $B_k$ . All other vertices are connected to the spine via legs in the same way as before.

□

Although the upper bound for the diameter of the graph is no longer constant as for disjoint compatible spanning trees, this statement is somehow stronger

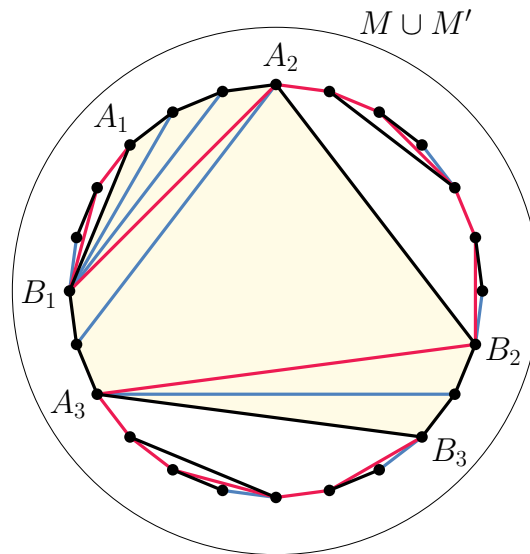


Figure 4.4: Union of two plane perfect matchings  $M$  and  $M'$  drawn in black with a symmetric difference of a single inside cycle containing three diagonals (shaded in gold) and a disjoint compatible caterpillar with red spine and blue legs.

in the sense that caterpillars are much more restricted than general spanning trees. Indeed, we can restrict them even further and demand that every vertex in those caterpillars has degree at most 3.

## 4.2 Disjoint compatibility via one-legged caterpillars

**Definition 4.5.** A caterpillar with maximum degree 3 is called a *one-legged caterpillar*. In the same way as before two plane perfect matchings  $M$  and  $M'$  on  $S$  are defined to be *disjoint compatible via one-legged caterpillars* if there exists a one-legged caterpillar  $C$  which is disjoint compatible to both  $M$  and  $M'$ .

**Definition 4.6.** The graph  $C_{2n}^*$  is defined as follows:

- the set of vertices is made up of all possible plane perfect matchings on  $S$
- two vertices are connected by an edge if and only if the respective matchings are disjoint compatible via one-legged caterpillars.

**Theorem 4.7.** For  $2n \geq 10$ , the graph  $C_{2n}^*$  is connected and  $\text{diam}(C_{2n}^*) = O(n)$ .

*Proof.* This proof works similarly to the proof for general caterpillars. For any two plane perfect matchings, we first consider the intermediate steps in the spanning tree setting, which number is bounded by four from above. Again, for each of those steps, we treat each inside cycle (which occurs in the symmetric difference of the two matchings) individually. However, we also need to break up each of those inside cycles into several 2-cycles.

This is done in the following way: Let  $\overline{A_1B_1}$  and  $\overline{A_2B_2}$  be two diagonals of the inside cycle. We assume for the moment that those are the only two diagonals of the inside cycle. By adding temporary diagonals starting in  $B_1$  as long as we do not exceed the diagonal  $\overline{A_2B_2}$ , we create a 'fan' of 2-cycles as depicted in Figure 4.5. The rest of the inside cycle is divided by a similar fan of temporary diagonals emerging from the endpoint of the last diagonal added from  $B_1$  (this is either  $A_2$  or its adjacent point along the inside cycle). By following this procedure, we obtain a chain of inside 2-cycles starting and ending at a diagonal.

If we have more than two diagonals on the inside cycle, we proceed as in the proof of Theorem 4.4 to generalise this procedure by considering all subcycles obtained by the spine separately and dividing them into 2-cycles in the same way.

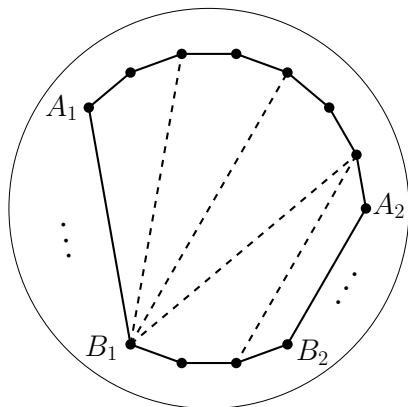


Figure 4.5: Subdivision of an inside 6-cycle into five inside 2-cycles.

Treating each occurring 2-cycle of each inside cycle on its own, we obtain in total again at most linearly many cycles. Therefore it is only left to show that there is a disjoint compatible one-legged caterpillar for any pair of matchings which obtains as symmetric difference exactly one inside 2-cycle.

As already mentioned, each 2-cycle is in fact an inside 2-cycle by construction of the chain, therefore the caterpillar can enter and leave the 2-cycle. All points outside the 2-cycle can be treated by the greedy approach described in the proof of Theorem 4.4. For the 2-cycle, several cases can occur as depicted in Figure 4.6.

If there are only two adjacent diagonals as in (a), the spine goes from the shared endpoint  $A$  of both diagonals in both directions to the respective endpoints  $B_1$  and  $B_2$ . The fourth point of the inside cycle is reached by a leg emerging from  $A$ .

If the only two diagonals are opposing as in (b), the spine goes from  $A_1$  to  $B_1$ , connects  $B_1$  to  $A_2$  within the cycle and continues until it reaches  $B_2$ .

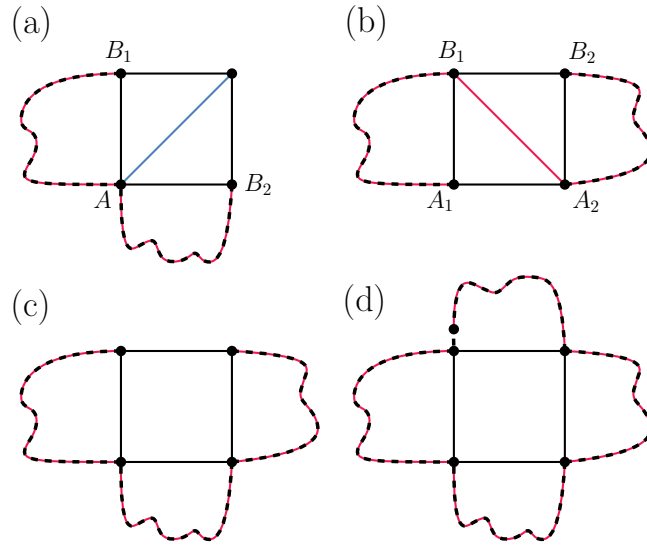


Figure 4.6: All possibilities for an inside 2-cycle (drawn as black square) with a disjoint compatible caterpillar sketched in colours (spine in red and legs in blue). (a) Two diagonals, they are adjacent. (b) Two diagonals, they are not adjacent, but opposing. (c),(d) There are three and four diagonals, respectively.

If the inside 2-cycle is surrounded by either three or four diagonals, the spine of the caterpillar goes around the inside cycle but never enters it, as shown in (c) and (d), respectively.

As shown for Theorem 4.4, the caterpillar obtained from the greedy approach has a maximum degree of at most 3, the degree of the starting vertex  $A$  is one and the degree of the endvertex  $B$  is at most 2. For each of the above cases, the total degree of the diagonals' endpoints is increased to at most 3. Therefore the total maximum degree of the disjoint compatible caterpillar is bounded by 3 as well.  $\square$

## 5 Conclusion

In this Master's thesis we considered different disjoint compatibility graphs on the set of all plane perfect matchings on  $S$ , where  $S$  is a set of  $2n$  points in convex position.

In Chapter 2, two plane perfect matchings are considered to be compatible if there exists a plane spanning tree which is disjoint compatible to both of them. We defined the notion of ears and inside cycles and showed that for two matchings with a symmetric difference of only inside cycles, the distance in the disjoint compatibility graph is 1. Furthermore, if the symmetric difference consists of a  $k$ -ear with  $k \geq 6$ , the distance is at most 3.

As the two main results we first proved in Theorem 2.9 that for at least ten points, the disjoint compatibility graph is connected and the diameter is upper bounded by 5. Second, in Theorem 2.18 we found two special matchings on the point set  $S$  of at least ten points, namely the two 2-semiear matchings for even  $n$  and the two near-2-semiear matchings for odd  $n$ , and showed that their distance in the disjoint compatibility graph is at least 4, thus the diameter of the graph is lower bounded by 4.

One open problem is to close the gap between 4 and 5.

In the third chapter, we analysed the disjoint compatibility of plane perfect matchings via plane Hamiltonian paths. It is an easy observation that not all matchings are connected via those paths. More precisely, many matchings – as those with at least three semiears – do not obtain any disjoint compatible Hamiltonian path. We defined a bipartite disjoint compatibility graph with all plane perfect matchings on one side and all plane Hamiltonian paths on the other side. We showed that both perimeter matchings have exactly

$\frac{n}{3}(2^{n-1} + (-1)^n)$  disjoint compatible Hamiltonian paths. For matchings with exactly two semiears, if and how many disjoint compatible paths exist depends on the size of the faces in between. If any face is too unbalanced, the matching is isolated in the compatibility graph, as well as all matchings consisting of only an odd number of parallel edges.

In Theorem 3.12 we finally showed that the two perimeter matchings themselves are not connected in the bipartite disjoint compatibility graph, therefore this graph is disconnected even when restricting to only non-isolated vertices.

Finally, in the fourth chapter, we restricted the intermediate disjoint compatible trees again, but in a way that the underlying compatibility graph is still connected for sufficiently many points. In detail, it was proven that all plane perfect matchings on at least ten points are connected via disjoint compatible caterpillar trees with maximum degree 3, also called one-legged caterpillars. The diameter of the respective disjoint compatibility graph is at most linear in  $n$ .

# List of Figures

1.1	Plane perfect matchings on 10 and 14 points, respectively, with no disjoint compatible plane perfect matching. . . . .	10
2.1	Two plane perfect matchings on the same set of twelve points in convex position (drawn in blue) which are disjoint tree-compatible. The complying disjoint compatible spanning tree is drawn in green. . . . .	12
2.2	The two perimeter matchings on a set of twelve points. The odd perimeter matching is drawn in blue and the even perimeter matching is drawn in red. . . . .	13
2.3	Left: A matching $M$ with two semicycles $X_1$ (red edges) and $X_2$ (blue edges) and their convex hulls. The corresponding cycle $\bar{X}_1$ is an inside 4-cycle, since the boundary of the red shaded area contains at least two (in fact three) diagonals. The cycle $\bar{X}_2$ is a 4-ear. Right: The matching $M'$ resulting from rotating the cycle $\bar{X}_1$ . . . . .	13
2.4	(a) Two plane perfect matchings on the same convex point set differing at a single inside cycle (shaded in red). (b) Triangulation of the cycle $C$ such that $u$ and $v$ are the only two ears. The added diagonals $D$ are drawn in purple. (c) Three outside parts $P_1$ , $P_2$ and $P_3$ (shaded) and the respective edge sets $M_1$ , $M_2$ and $M_3$ (coloured). (d) Triangulation $T_i = M_i \cup A_i$ of the outside parts; the added edges $A_i$ are drawn in purple. (e) The union of $D$ and all $A_i$ results in a planar spanning graph which contains a spanning tree (depicted in (f) in pink). . . . .	15
2.5	Intermediate steps for the rotation of a $k$ -ear with $k \geq 6$ . . . . .	16



List of Figures

---

2.6	Rotation of a 6-ear in 3 steps (in each step we rotate the grey inside cycle). . . . .	16
2.7	Schematic depiction of the whole graph $G_{10}$ . The letter $r$ stands for a possible rotation by $2\pi/10$ . Going against the arrows rotates in opposite direction. Next to each vertex, the number of different matchings resulting from rotations is indicated. The edges indicate either the rotation of an inside cycle (in gray), or a compatible spanning tree (red). . . . .	17
2.8	All matchings are sufficiently close to the blue (odd) perimeter matching $B$ and/or to the red (even) perimeter matching $R$ . . .	18
2.9	For a fixed matching $M$ , we colour the perimeter edges alternately in blue (odd edges) and red (even edges). The colouring extends to a proper colouring of a tree $D(M)$ that is dual to $M$ . In the shown example, rotating the inside cycle corresponding to the blue interior node of $D(M)$ creates a tree which leaves all have the same colour. . . . .	19
2.10	When $b \geq 2$ and $r = 1$ we can get to $B$ in 2 steps and to $R$ in 3 steps. . . . .	19
2.11	Intermediate steps for the case $b = 1$ and $r = 1$ . . . . .	20
2.12	Boundary areas with five points (left) and four points (middle). The drawing on the right does not show a boundary area; not all points are neighbouring on the convex hull of $S$ . . . . .	22
2.13	Left: A 2-semiear matching. Right: A near-2-semiear matching.	22
2.14	Two matchings $M$ and $M'$ (depicted in red and blue) creating an ear. The points $p_1$ and $p_2$ might be connected by a spanning tree outside the ear. . . . .	23
2.15	An (even) 2-semiear matching drawn in red and a blue matching with at least one odd perimeter edge; on the left the blue matching creates a cycle with the red matching, on the right a boundary area with three points occurs. . . . .	24
2.16	All possible cases for a semiear of size $k \geq 3$ in a matching $M$ (depicted in red) and a second matching $M'$ (depicted in blue) which does not use any of the perimeter edges in $M$ . . . . .	26

List of Figures

---

2.17	All possible cases for a 2-semiear in a matching $M$ (depicted in red) and a second matching $M'$ (depicted in blue) which does not use the perimeter edges in $M$ . . . . .	27
2.18	An even 2-semiear in $M$ (red matching edges) intersected by two diagonals in $M'$ (blue edges) (on the left) and an odd 2-semiear in $M'$ intersected by two diagonals in $M$ (on the right). The vertices $u$ and $v$ might coincide. The grey areas are blocked, that is, the spanning tree cannot pass them. Therefore, at least three points (if $u = v$ ) are not reachable from the rest of the vertices (marked by white crosses). . . . .	28
2.19	Illustrations, that the distance between two special 2-semiear matchings (left) and between two special near-2-semiear matchings (right) is at least 4. Even perimeter edges are drawn in red, odd ones are drawn in blue. The numbers next to the edges indicate which Lemma is applied. Crossed out edges indicate that this type of edge (even or odd) cannot appear in that matching. . . . .	29
3.1	A $k$ -semiear in a plane perfect matching with a possibly disjoint compatible path drawn in green entering the ear at $v_1$ and leaving it at $v_{2k}$ . If the path reaches vertex $v_i$ , it can only traverse vertices with index either smaller or larger than $i$ afterwards. . . . .	33
3.2	For a fixed point $p$ there are three possible starts for a path on $n$ perimeter matching edges (top row). They can recursively be continued on sets with $n - 1$ , $n - 2$ , and again $n - 2$ matching edges, respectively. . . . .	35
3.3	A plane perfect matching $M$ on $S$ with two semiears, two faces and their convex hulls. A $(0, 2)$ -face $F_1$ is drawn in blue and a $(2, 3)$ -face $F_2$ is depicted in red. . . . .	36
3.4	The four different ways of a path visiting the two endpoints of a diagonal, here drawn in black. In the two figures on the left, the path meets one of the points before crossing to the second face, that is, within the first face. In the two figures on the right, the path first traverses to the second face and only afterwards visits the second incident point of the diagonal. . . . .	37

List of Figures

---

3.5	There is no disjoint compatible Hamiltonian path meeting all points of a $(k, 2k + 3)$ -face: even if we try to visit as many point on the upper arc of the convex hull as possible, the path (drawn in red) misses at least two points and therefore cannot leave the face. . . . .	38
3.6	A $(2, 6)$ -face as an example for a $(k, 2k + 2)$ -face with a unique disjoint compatible Hamiltonian path drawn in red. The circles indicate which point on the smaller side with $2k + 2 = 6$ points saturates which two points on the larger side. The leftmost and rightmost points are those where the path is entering and leaving the face, respectively. . . . .	39
3.7	A $(k, 2k+2)$ -face with its unique disjoint compatible Hamiltonian path depicted in red (dashed). Deleting one matching edge on the upper arc (crossed in blue) yields a $(k, 2k+1)$ -face. There are three different ways for a disjoint compatible Hamiltonian path to run in this face as depicted in green. The points encircled in green are visited by the path outside of the face. . . . .	40
3.8	(I) Two different disjoint compatible paths for a 2-semiear. They meet both endpoints of the diagonal within the semiear and leave either above or below. (II) For a semiear with at least three perimeter edges, any variant of a disjoint compatible path is feasible. . . . .	41
3.9	All possible kinds of disjoint compatible paths in a $(k, 2k)$ -face, depicted for $k = 1$ . . . . .	43
3.10	All possible kinds of disjoint compatible paths in a $(k, 2k - 1)$ -face, depicted for $k = 2$ . . . . .	44
3.11	All possible kinds of disjoint compatible paths in a $(k, l)$ -face for $2 \leq k \leq l \leq 2k - 2$ , depicted for $k = l = 2$ . . . . .	45
3.12	All possible kinds of disjoint compatible paths in a $(0, 0)$ -face. . . . .	46

## List of Figures

---

3.13	A plane perfect matching with two semiears on a set of 44 points in convex position. The semiears and faces are depicted in different colours. For each diagonal, it is indicated which options for a disjoint compatible Hamiltonian path are feasible. All values provided with a tilde refer to the reflection of the respective face across the horizontal axis. The set of feasible interactions of a path with the diagonals is not empty at any point. For a 3-semiear as in this example on the right, any option is valid. Therefore a (not necessarily unique) disjoint compatible Hamiltonian path exists; one of them is indicated in grey and the respective options chosen at the diagonals are highlighted in blue. If the semiear on the right was a 2-semiear, then no disjoint compatible path would exist since this would require either option (c) or (d) for the rightmost diagonal. . . . .	47
3.14	A plane perfect matching consisting of an odd number of parallel matching edges. The faces have to be treated alternately, therefore a parity conflict arises and there is no possibility to draw a disjoint compatible Hamiltonian path. . . . .	48
3.15	Two matchings creating a boundary area with two points. . . .	49
4.1	A (spanning) caterpillar on a convex set of 14 points. The spine is depicted in red, the legs are drawn in blue. . . . .	55
4.2	A disjoint compatible caterpillar from $A$ to $B$ with maximum degree 3. The spine is depicted in red, the legs are drawn in blue. . . . .	56
4.3	Union of two plane perfect matchings $M$ and $M'$ drawn in black with a symmetric difference of a single inside cycle containing two diagonals (shaded in gold) and a disjoint compatible caterpillar with red spine and blue legs. . . . .	57
4.4	Union of two plane perfect matchings $M$ and $M'$ drawn in black with a symmetric difference of a single inside cycle containing three diagonals (shaded in gold) and a disjoint compatible caterpillar with red spine and blue legs. . . . .	58
4.5	Subdivision of an inside 6-cycle into five inside 2-cycles. . . . .	60

List of Figures

---

- 4.6 All possibilities for an inside 2-cycle (drawn as black square) with a disjoint compatible caterpillar sketched in colours (spine in red and legs in blue). (a) Two diagonals, they are adjacent. (b) Two diagonals, they are not adjacent, but opposing. (c),(d) There are three and four diagonals, respectively. . . . . 61

# List of Tables

- 3.1 All valid output cases of the algorithm for a given  $(k, l)$ -face with the respective input case. If the input contains several cases, then the output is the union of the corresponding entries in the table. . . . . 46
- 3.2 Key values for the bipartite graph  $B_{2n}$  such as the number of matchings and paths in total (which is the number of vertices in  $B_{2n}$ ) as well as the number of components with matchings and isolated paths for  $n = 1, \dots, 11$  obtained by computer calculations. 52

# Bibliography

- [1] Oswin Aichholzer, Andrei Asinowski, and Tillmann Miltzow. Disjoint compatibility graph of non-crossing matchings of points in convex position. *The Electronic Journal of Combinatorics*, 22:1–65, 2015. URL: <http://www.combinatorics.org/ojs/index.php/eljc/article/view/v22i1p65>.
- [2] Oswin Aichholzer, Sergey Bereg, Adrian Dumitrescu, Alfredo García, Clemens Huemer, Ferran Hurtado, Mikio Kano, Alberto Márquez, David Rappaport, Shakhar Smorodinsky, Diane L. Souvaine, Jorge Urrutia, and David Wood. Compatible Geometric Matchings. *Computational Geometry: Theory and Applications*, 42(6-7):617–626, 2009.
- [3] Oswin Aichholzer, Julia Obmann, Pavel Paták, Daniel Perz, and Josef Tkadlec. Disjoint tree-compatible plane perfect matchings. *Proceedings of EuroCG*, pages 398–405, 2020.
- [4] Oswin Aichholzer, Julia Obmann, Daniel Perz, Josef Tkadlec, and Birgit Vogtenhuber. Edge-disjoint matching-path-matching for convex point sets. *Manuscript*, 2020.
- [5] Oswin Aichholzer, Julia Obmann, Daniel Perz, and Birgit Vogtenhuber. Edge-disjoint matching-caterpillar-matching for convex point sets. *Manuscript*, 2020.
- [6] Carmen Hernando, Ferran Hurtado, and Marc Noy. Graphs of non-crossing perfect matchings. *Graphs and Combinatorics*, 18(3):517–532, 2002.
- [7] Michael E. Houle, Ferran Hurtado, Marc Noy, and Eduardo Rivera-Campo. Graphs of triangulations and perfect matchings. *Graphs and Combinatorics*, 21(3):325–331, 2005.

## Bibliography

---

- [8] Mashhood Ishaque, Diane L. Souvaine, and Csaba D. Tóth. Disjoint compatible geometric matchings. *Discrete & Computational Geometry*, 49(1):89–131, 2013.
- [9] Andreas Razen. A lower bound for the transformation of compatible perfect matchings. *Proceedings of EuroCG*, pages 115–118, 2008.
- [10] Neil J. A. Sloane. *The On-Line Encyclopedia Of Integer Sequences*. URL: <http://oeis.org/A001045>.